65158

AUGUST

1965

ROYAL AIRCRAFT ESTABLISHMENT

TECHNICAL REPORT No. 65158

CORROSION FATIGUE AND STRESS CORROSION CRACKING OF AN ALUMINIUM-5°/o MAGNESIUM-4°/o ZINC ALLOY TOTALLY IMMERSED IN 3°/o NaCℓ AND OTHER CORRODENTS

by

P. J. E. Forsyth

E. G. F. Sampson

MINISTRY OF AVIATION
FARNBOROUGH HANTS

U.D.C. No. 669.715.721.5 : 620.194.8 : 620.194.2 : 620.193.27 : 539.219.2

ROYAL AIRCRAFT ESTABLISHMENT

Technical Report No. 65158

August 1965

CORROSION FATIGUE AND STRESS CORROSION CRACKING OF AN ALUMINIUM-5% MAGNESIUM-4% ZINC ALLOY TOTALLY IMMERSED IN 3% NaCl AND OTHER CORRODENTS

by

P. J. E. Forsyth
E. G. F. Sampson

SUMMARY

Corrosion fatigue and stress corrosion tests have been done on aluminium-5% magnesium-4% zinc alloy in two conditions of heat-treatment, i.e. aged to peak hardness at 120°C and at 150°C.

The frequency used for most of the fatigue tests was 20 c/min, but comparisons have been made at frequencies of 180 and 1500 c/min. The fatigue endurance at 20 c/min changed only a small amount over a large range of stress. The S/log n curve showed a clearly defined 'knee' and fatigue limit.

All crack paths were intercrystalline under both corrosion fatigue and stress corrosion conditions, although air fatigue cracks in this material are mainly transcrystalline.

The slopes of the S/log n curves for 20 and 180 c/min were similar, but the 1500 c/min curve had a smaller slope. This difference was clearly associated with the 'knee' in the 20 c/min curve that was not evident at the higher test frequency.

The effects of both anodic and cathodic polarization have been studied. Marked changes in crack growth rate were observed when a fatigue specimen was

alternately made anodic and cathodic in a 3% NaCℓ solution against either a platinum or aluminium electrode with an externally impressed current. Similar changes in crack growth rate could be obtained with impressed currents under steady stress corrosion conditions. Stress corrosion crack growth rates have been shown to be dependent on the chloride ion concentration of electrolytes used, suggesting a metal dissolution mechanism of stress corrosion in this material.

Departmental reference: CPM 33

CONTENTS

1 INTRODUCTION

Certain peculiarities of fatigue behaviour of the ternary aluminium-magnesium-zinc alloy with 5% magnesium and 4% zinc had suggested that this composition was unique, within the range of compositions tested, as regards its fatigue behaviour[1,2]. The prime feature was that its grain deformation was very homogeneous under all forms of fatigue stressing, and additionally, torsional fatigue failure was wholly intercrystalline. Later work by Stubbington[3] demonstrated that this torsional fatigue behaviour was not unique, but depended on what had been an arbitrary choice of ageing temperature (150°C) for the earlier work. By ageing at 120°C the alloy now behaved in a manner we have found to be typical of the aluminium 7.5% zinc 2.5% magnesium alloy. The characteristics of this alloy were the formation of coarse slip striations, and eventually the occurrence of transcrystalline cracking along these striations. Further, it was possible to induce fine, homogeneous slip deformation in the latter alloy by ageing at 240°C or at 150°C for a considerable period of overageing.

Having established this ageing temperature-fatigue behaviour relationship it was considered necessary to study the corrosion fatigue behaviour of the Al-5% Mg-4% Zn alloy in the two conditions of heat treatment that gave different deformation and cracking characteristics, i.e. aged to peak hardness at 120°C and at 150°C.

There was reason to believe that the 150°C ageing treatment that resulted in grain boundary air fatigue under torsional stress would also result in grain boundary failure under 3% NaCl solution in other forms of fatigue stressing, and the 120°C ageing treatment might give a transcrystalline corrosion fatigue fracture characteristic of the Al-7.5%Zn-2.5%Mg alloy. If the two forms of corrosion fatigue could be obtained in the same alloy composition it was hoped that further information might be obtained regarding the connection between corrosion fatigue and stress corrosion, the latter phenomenon being exclusively intercrystalline in these alloys. Information was also sought on the effects of anodic and cathodic polarization on the rate of crack growth, and the local behaviour of the crack tip. As will be described in the body of the report, no transcrystalline corrosion fatigue cracks were observed in this work, except when cracks were growing rapidly at high stress.

Earlier work on fatigue fracture features led to considerations of the effects of frequency on crack growth increments, and the general form of

cracks subject to an active environment for different times during the fatigue cycle. To study this it was considered necessary to do fatigue tests at three frequencies, 20, 180 and 1500 c/min.

2 EXPERIMENTAL

2.1 Material

The alloy was made from high purity metals, chill cast, no grain refining additions were used. After upsetting and forging of the ingot the material was scalped and rolled to 0.064" strip from which 'B' size tensile test pieces were cut. All specimens were electrolytically polished before testing.

Test pieces were solution heated for 1.25 hours at 470°C in a salt bath, cold water quenched, and subsequently aged to peak hardness at either of the selected temperatures 120°C and 150°C.

2.2 Fatigue testing machine

An Avery-Schenck reverse plane bend machine was modified to accept a vertically disposed test piece of a form suitable for total gauge length immersion in the corrodent. This was achieved by the modifications shown in Figs.1 and 2.

Two steel brackets A and B were bolted to the existing specimen grip positions. The specimen was bolted to bracket B the free end sliding unconstrained between the rollers on bracket A Thus the specimen was loaded as a simple cantilever with a horizontal application of load to the free end. For large amplitudes the position of application of the load shifted slightly, but this led only to a minor error in stress measurement at high stresses. For convenience the specimens were formed from standard 'B' size tensile test pieces modified by reducing the width of their free ends for insertion between the rollers. As will be described later, the same type of test piece was used in the bending stress corrosion rig. The new fatigue arrangement was calibrated by horizontally loading the bracket A at the position of the rollers, and measuring the beam deflection at the dial gauge.

The standard speed of this machine is 1500 c/min. For use at lower frequencies, a separate motor/gear box with a continuously variable ratio ('Kopp' gear box) was used with a belt drive from its output pulley to another pulley attached behind the existing flywheel on the machine. Thus when running at low frequency the existing motor behaved as a layshaft. The dashpot controlled 'cut out' would not operate satisfactorarily at low frequencies, nor

was the counter suitable for low frequency low cycle endurance tests. For these reasons it was necessary to arrange for specimen fracture to release a micro-switch so that the test could be timed. This arrangement can also be seen in Figs.1 and 2.

For some of the work at 20 c/min an inductance transducer was used in conjunction with a 'Graphispot' recorder. By using this arrangement the growth rate of cracks could be determined by amplitude reductions resulting from loss of stiffness in the specimen. The loss of stiffness could result from the growth of one or many cracks, and therefore it was not possible to directly calibrate this property with crack length. However, it was possible to relate the behaviour of the specimen to that of a standard specimen that had been stressed with 'equivalent' cracks of different depths. These cracks were made by a carefully controlled saw cut. A plot of saw cut depth against load loss was used as a rough indication of ℓ or effective crack depth in the corrosion fatigue tests. The crack growth rates plotted by this method were accurately substantiated by fracture striation spacing measurements.

2.3 STRESS CORROSION TEST APPARATUS

A four position stress corrosion test rig was constructed that allowed accurate timing of test endurance. The rig is shown in Fig.3. The bending moment is applied through a lever arm with dead weight loading. When the specimen fractures the lever drops and closes a microswitch, thus stopping the recording clock. An inductive transducer was used to measure movement of the lever arm thus detecting crack initiation and following growth. As with the cyclic tests a calibration curve of saw cut depth, i.e. equivalent crack depth against lever deflection was obtained. It was found that up to $\simeq$ 0.030" cut depth the lever deflection (as measured with the transducer and Graphispot recorder) was linear. From this curve crack lengths and growth rates could be stated in terms of inches and inches/min.

3 CORROSION FATIGUE AND STRESS CORROSION TESTING PROCEDURE

The plane bend test pieces described earlier were tested under total immersion conditions using initially 3% NaCℓ solution, and later in the work various concentrations of HCℓ in water. This was arranged by partially enclosing the vertically disposed specimen in a P.V.C. tube or for the stress corrosion work in a glass container. Lower end sealing was obtained by clamping the P.V.C. tube to the lower or fixed end of the specimen with a laboratory tube clip. The glass container was sealed at its lower end by

casting a 'fleximold' plug of the requisite shape. Both types of container were partially filled with the electrolyte. The area of specimen totally immersed in the liquid was 8 cm^2 and the waterline was protected with 'Lacomit' varnish.

For those experiments where impressed currents were employed a thin platinum strip with approximately the same surface area was immersed in the solution facing the electrolytically polished surface of the fatigue specimen. For the later work on stress corrosion a totally surrounding electrode was used. The necessary current density could be maintained by manual adjustment of the external voltage supplied through a potentiometer, although in some of the experiments the cell current was allowed to fall to the normal polarized level, and the current/time curve recorded.

4 CORROSION FATIGUE TESTS: REVERSE PLANE BEND TOTALLY IMMERSED IN 3% NaCl SOLUTION

Fig.4 shows stress/log n curves for aluminium 5% magnesium 4% zinc aged at 150°C for 4 days, tested at three frequencies 20, 180 and 1500 c/min. Several test points for cathodically and anodically polarized specimens are included. All specimens were electrolytically polished over their gauge length which was completely immersed in the corrodent.

The lower frequency curves (2 c/min and 180 c/min) have abrupt 'knees' at a fatigue limit of $\simeq \pm 2.5$ T/in^2 and endurances of 2×10^3 and 7×10^3 cycles respectively. It will be noticed that the life is approximately the same over the steep part of the two curves for the 20 and 180 c/min tests as shown by their similar slopes.

Fig.5 shows similar curves for the same material aged at 120°C for 10 days. The curves and their related dispositions are similar to those for the 150°C ageing temperature. Fig.6 shows the tensile stress/strain curves for the two heat treatments and the relation of these properties to fatigue strength will be discussed later.

5 STRESS CORROSION TESTS: PLANE BENDING TOTALLY IMMERSED IN 3% NaCl SOLUTION

Fig.7(a) shows stress/time curves for the two conditions of heat treatment, and 7(b) the relation between steady and cyclic stress lives. These curves show that on a time base as opposed to the number of cycles plot the lives are similar with a threshold stress of $\simeq 3$ T/in. However marked scatter was experienced with

the low ageing temperature material under steady stress corrosion. This scatter was greater than that experienced with the 150°C ageing temperature material under stress corrosion and of the fatigue tests. Crack growth rate experiments are described later in this report.

6 CRACK GROWTH RATES UNDER CORROSION FATIGUE CONDITIONS

Cracks observable by the presence of gas bubbles and associated corrosion product occurred in the very early stages of the specimen life, and it was required to obtain more information on the rates of crack growth that occurred. In view of the shape of specimens this could not be done directly, and an estimate was obtained by recording the loss of stiffness of the specimen during the test. In the type of test used the load drops as the section is reduced by a crack. A calibration specimen, as described earlier, was used to determine crack depth. The curve relating percentage load drop/crack length is given in Fig.8.

By the use of the transducer and 'Graphispot' recorder it was possible to plot the amplitude swing i.e. the load level per cycle and follow the rate of drop of peak load. It was found that although corrosion fatigue lives for the two heat treatments were similar the rate of crack growth was initially slower and later faster for the low ageing temperature condition. By the use of this data and the calibration curve a $\frac{d\ell}{dn}$ v ℓ curve was obtained as shown in Fig.9. This clearly indicates the difference in crack growth rate obtained with the two conditions of heat treatment.

7 EXPERIMENTS WITH EXTERNALLY IMPRESSED CURRENTS. CORROSION FATIGUE AT 20 C/MIN

As mentioned earlier the method used for these experiments was to arrange a platinum electrode in the close vicinity of the stressed surface of the specimen. The steady current density chosen for protection experiments where the specimen was made a cathode was 50 $\mu A/cm^2$, and where polarity reversal was used the anodic current density was initially 100 $\mu A/cm^2$ obtained by direct switching of the external power source. A 'Graphispot' plot of cyclic load drop i.e. a plot of the peak cycle values against time gives crack growth rates changing with impressed current as shown in Fig.10.

The effect of a continuously impressed protective current density of 50 $\mu A/cm^2$ was to extend the life of the specimen indefinitely, whereas the anodically polarized specimens failed in about 1/10 of their normal corrosion fatigue life. These features are indicated on the S/log n curves in Figs.4 and 5. Where complete protection by cathodic polarization was achieved, no

cracks were ever observed, and the specimen surface became uniformly coated by a translucent hydroxide film as shown in Fig.11. Here the film can be seen and brittle cracks in the film are continuous over the exposed boundaries, arrow A. A microsection through a typical area shows that an open mouthed cavity had developed at the exposed boundary presumably by local action, but no further crack extension was ever observed. This is shown in Fig.12. If cracks were allowed to form by normal corrosion fatigue, or even encouraged to form by anodic polarization, protection could be applied and the rate of growth enormously reduced by subsequent cathodic polarization.

8 CRACK GROWTH RATE EXPERIMENTS UNDER STEADY STRESS CORROSION CONDITIONS

Stress corrosion cracking could be followed in a way similar to that described for the fatigue experiments, and crack growth curves ℓ/t were plotted with the 'Graphispot' recorder. Fig.13 illustrates the effect of various levels and polarity of the impressed current on stress corrosion crack growth rate. As with the cyclic stress tests cracking was sensitively affected by impressed currents, and instantaneous protection was afforded by current densities as low as 50 $\mu A/cm^2$ whereas polarity reversal making the specimen an anode with respect to the platinum electrode, greatly increased the crack rate. There were three interesting points worthy of notice

(1) Even a short period of cathodic protection could afford prolonged protection after switching off the current.

(2) A more prolonged period of cathodic protection could afford extended protection even though the specimen might be subjected to an intermediate period of anodic attack where the crack was observed to spread rapidly.

(3) An early period of anodic attack, even though followed by a period of cathodic protection, resulted in a rapid crack rate commensurate with the anodic rate where the current was switched off.

These effects could be explained by the different neutralization times for the external electrolyte conditions and the electrolyte at the tip of the growing crack, e.g. an early period of cathodic protection produces an alkaline condition at and near the specimen surface and within the crack. A change in polarity causes an immediate change of pH in the main volume of the solution near and at the specimen surface, but not necessarily at the crack tip unless the initial alkalinity was maintained only for a short time. If the initial cathodic time was long then any small acidic volume developed by subsequent anodic treatment

is on switching off rapidly neutralised by the very much larger alkaline volume still persisting and crack growth is halted. Similarly if an early acidic condition is set up at the specimen surface and within the crack by a period of anodic treatment, a short period of cathodic treatment can halt the crack but provide no subsequent protection when the current is switched off.

9 CRACK GROWTH RATE DETERMINATIONS WITH VARIOUS CONCENTRATIONS OF HCℓ

Stress corrosion tests were carried out as previously described but now using various fractions of normal HCℓ solution and plotting complete crack growth curves. In order to more completely standardize the conditions at the crack tip an anodic current of 100 $\mu A/cm^2$ was maintained on the totally immersed specimens. From this crack growth data, growth rate $\left(\frac{d\ell}{dt}\right)$ values were plotted against HCℓ concentrations for similar crack lengths and against crack length itself. This data is shown for the two standardized conditions of heat treatment i.e. 10 days at 120°C and 4 days at 150°C. Fig.14 shows the $\frac{d\ell}{dt}$ v HCℓ concentration curves for material aged at 120°C and Fig.15 shows similar curves for material aged at 150°C. Fig.16 compares two concentrations 0.0001 and 0.01 N, for the two alloys. Figs.14 and 15 illustrate the reduction in stress corrosion crack growth rate with concentration, approaching zero growth rate for very dilute solutions and for very short cracks, but revealing an additional stress cracking effect appearing at longer crack lengths. Fig.16 can be compared with Fig.9 i.e. that the material aged at 120°C starts cracking more slowly than the 150°C aged material, but as the crack deepens the growth rate increases and exceeds that of the 150°C aged material. This behaviour is confirmed with reference to the stress/time curves shown in Fig.7 where it can be seen that the lower ageing time gives a higher threshold stress, but shorter lives at higher stresses. It is also evident from this data that crack growth rates are, over a large range of crack length more rapid for the very dilute electrolytes although the lives will be very much greater.

The fact that those test conditions that prolonged the test also resulted in more rapid final growth was of some further interest. It appeared that the grain boundaries were conditioned to a greater susceptibility after prolonged loading, and to check this point specimens were loaded for 96 hours in air and then, without removing the stress, the electrolyte was added and the impressed current switched. Fig.17 shows that pre-stressed material although initially cracking more slowly eventually cracks more rapidly than normal material. These tests were done at 7 T/in^2 in 0.0001 N HCℓ with an impressed anodic current of 0.4 mA, i.e. 50 $\mu A/cm^2$.

10 SUPERFICIAL OBSERVATIONS ON FAILED SPECIMENS

All failures produced by corrosion fatigue and stress corrosion in both conditions of heat treatment were intercrystalline with the exception of the last portion of the corrosion fatigue fractures. High frequencies and high fatigue stresses both caused a slight increase in the amount of final transcrystalline failure. The material aged at 150°C always exhibited a large number of initial cracks in 3% NaCℓ solution whether it was subjected to corrosion fatigue or stress corrosion whereas the 120°C aged material sometimes failed from a solitary crack.

At low stresses long endurances some evidence of general corrosion was found although the fracture surfaces were always remarkably bright. The surface corrosion was, in general, only noticeable in the vicinity of growing cracks.

11 METALLOGRAPHIC OBSERVATIONS

Crack initiation

Corrosion fatigue crack origins at grain boundaries were accompanied by extruded debris as shown in Figs.18 and 19. This extruded material appeared to be of a crystalline nature (probably thin ribbon like oriented crystals) that showed optical anisotropy under polarized light. Direct replication with evaporated carbon successfully extracted some of these debris streamers, and also replicated the surface pits along the grain boundaries as shown in Fig.19.

Stress corrosion cracks also originated at grain boundaries under all observed conditions in both heat treatment conditions and as with the corrosion fatigue specimens the 150°C aged material exhibited many more cracks than the 120°C aged material. Unlike the corrosion fatigue specimens no extruded debris was found although a typical cathodic film was formed at a distance from the mouth of each crack as shown in Fig.20.

12 FRACTOGRAPHIC OBSERVATIONS

Corrosion fatigue

As already mentioned both corrosion fatigue and stress corrosion cracks were predominantly intercrystalline. This was most clearly revealed by fractographic examination where specular boundary facets were usually observed.

At relatively high corrosion fatigue stresses grain boundary growth striations were revealed. The striation spacing and the height were observed to increase with increasing stress, and therefore were usually most pronounced

in the final fracture region. In this respect little distinction could be drawing between the material in the two conditions of heat treatment, although it appeared that the low ageing temperature material showed less pronounced striations.

The grain boundary striations were free from river patterns that characterise transcrystalline corrosion fatigue facets. As might be expected the river patterns seemed to be peculiar to crystallographic crack growth. The grain boundary striations had a marked similarity to ductile striations, and from various observations it was concluded that the ridge of any striation on one half of the failure would mate with the groove of the corresponding striation on the other half. This being so it was clear that these striations were similar in form to the transcrystalline ductile striations commonly observed in aluminium alloys, and were not formed by the mechanism suggested by Smith and Laird[4], but rather they were formed by a crack tip that was wavering in its growth direction. In order to obtain some quantitative values relating to the contour of the striations a typical surface was studied with multiple beam interferometry using a 'Linnick' microscope. Figs.21 and 22 show a direct optical micrograph and its equivalent interferogram from which it is concluded that the striations have the form indicated in Fig.23. By referring to the features of typical grain boundaries in this material we find that the precipitate denuded zone width is of the same order of magnitude as the crack tip deviation i.e. $\simeq 0.25$ micron.

13 FRACTURE FEATURES UNDER CORROSION FATIGUE CONDITIONS WITH IMPRESSED CURRENTS

The striations observed on corrosion fatigue fractures where changes in polarity of the impressed current have been made are shown in Figs.24 and 25. In Fig.24 a regular change of polarity was made every 10 stress cycles and the marked change in growth rate can be seen from the changes in striation spacing. Thus when the specimen was protected the crack growth was very small and with anodic polarization the growth rate increased many times. These growth rates correlated numerically with the rates obtained from the calibration. Fig.25 shows similar groups of striations and indicates the shape of the crack front as it extended across the grain boundary.

14 FAST FRACTURE OBSERVATIONS

A peculiarity of the fracture of the low temperature aged material ($120^{\circ}C$) was that numerous kink bands developed during the rapid final growth

period. These are shown in Fig.26(a) and (b) where two mating facets are illustrated and again in Fig.27 where the surface tilts are clearly revealed. No similar features were found in the 150°C aged material. Similar kink bands could be developed on impact fractures in the low ageing treatment material. In addition to these fast fracture features cleavage facets have been developed in the final fracture phase of this material as shown in Figs.28 and 29.

15 DISCUSSION

The shapes and relative dispositions of the S/N curves for the three different frequencies show that the two conditions of heat treatment, i.e. 120°C and 150°C, give remarkably similar properties, and are similarly affected by testing at the various frequencies. If one examines the displacement of the 20 and 180 c/min curves it can be seen that over the range of stress used fatigue life in terms of cycles is increased by a factor of 4 with a reduction of cycle period by a factor of 9.

These endurances are presented in terms of time in Fig.7(b) where they are superimposed on the stress corrosion/time curve for the 150°C aged material. The endurance n is converted by taking the total time that the specimen is subjected to a positive stress above a certain threshold value, in this case derived from the stress corrosion curve as 3 T/in^2. This appears to be justified as most of the endurance is crack propagation and this commonly occurs mainly from one side of the plane bending specimen.

The results of the experiments with impressed currents show clearly that the growth rate of cracks whether resulting from a steady positive stress or a cyclic stress is strongly dependent on the polarity and current density applied. Referring in all cases to cracks that follow the grain boundaries, then cathodic currents even of a level as low as 50 μA/cm^2 can fully protect the specimen. In addition, these cathodic currents can impart protection after switching off. Conversely anodic currents cause accelerated crack growth, and the reversal of polarity can produce an instantaneous change in growth rate. It is interesting to note that prolonged periods of cathodic protection if applied before any anodic treatment can confer extended and instantaneous protection on switching off after an inserted period of anodic attack. This suggests, as mentioned earlier, that the pH of the crack tip electrolyte changes rapidly by diffusion and neutralization down the crack.

The experiments using electrolytes of varying concentration of HCℓ in water where in all cases an anodic current density of 100 μA/cm^2 was used,

show that crack growth rate is dependent on the chloride ion concentration at the crack tip which seems to suggest a dissolution mechanism involving $3\,Cl^- + Al^{+++}$.

At very high cathodic current densities where accelerated growth occurred it was concluded that this is very possibly the result of hydrogen gas evolution within the crack causing an increase in crack tip stress.

The very dilute HCl concentrations result in prolonged specimen lives with the eventual formation of cracks that then proceed to grow more rapidly than in the more concentrated solutions. Conversely, more concentrated solutions cause earlier cracks to form and slower growth rates than in the dilute electrolytes. Although there is a definite tendency for more numerous cracks to form in concentrated electrolytes it was not considered that this was a factor in the case shown in Fig.16 where electrolyte concentrations of 0.0001 N and 0.01 N were used and the number of cracks involved in both electrolytes was about the same. Thus, there appears to be an effect of prolonged loading in producing an initial crack growth resistance and later easier crack growth. Further work is proposed on this effect.

16 CONCLUSIONS

(1) The repeated application of a stress, in what might be considered as a corrosion fatigue environment, can cause intercrystalline cracking that is indistinguishable from stress corrosion cracking in this alloy. All of the evidence suggests that the mechanism of crack growth is also the same.

(2) Only at relatively high crack tip stresses did the fracture appearance of the two types of loading differ where the cyclically loaded specimens exhibited fracture striations.

(3) In air, or at high stresses and frequencies where rapid cracking occurred, the fracture occasionally became transcrystalline.

(4) Clear evidence of cleavage fracture was found when cracked stress corrosion specimens were subsequently broken in air.

(5) If the specimen was made a cathode with respect to a platinum electrode by an externally impressed current immediate and complete protection was achieved. Growing cracks whether under a steady or cyclic stress were halted.

(6) Extended immunity to cracking was conferred by a short period of cathodic protection.

(7) Periods of anodic attack although causing immediate increase in crack growth rate had no permanent effect after removal of the current.

(8) Cathodic protection could be effective in providing prolonged immunity after removal of the current even if an intervening period of anodic attack had occurred.

(9) All of the evidence obtained from the various experiments suggests that crack growth in the Al-5%Mg-4%Zn alloy under both conditions of heat treatment, is a metal dissolution process at the crack tip, and this occurs when anodic conditions prevail. No evidence of a hydrogen embrittlement accelerated growth process was detected, and hydrogen only played a part when evolved rapidly enough to raise the gas pressure in the crack and thus apply an increased stress to the crack tip.

(10) There is evidence that environmental conditions causing extended lives result in fast final crack growth. Thus preloading a specimen in air can result in reduced stress corrosion cracking rates although a more rapidly accelerating final crack growth than observed in normal material.

(11) Differences in mechanical properties resulting from different ageing treatments result in minor but important differences in stress corrosion behaviour. High proof strength material has a higher threshold stress for stress corrosion, but shows shorter lives at high stresses. High proof strength material appears to develop fewer initial cracks, but the growth rates tend to be higher.

REFERENCES

No.	Author	Title, etc.
1	I.J. Polmear	Fatigue properties of ternary aluminium-zinc-magnesium alloys. Nature, Vol 183, pp 1388-1389, May 1959
2	R.W. George P.J.E. Forsyth	The influence of nickel and manganese on the fatigue properties and microstructures of three aluminium-magnesium-zinc alloys. R.A.E. Tech. Note No. Met Phys 352, 1962
3	C.A. Stubbington	Written discussion to the Fatigue and Creep session of the conference on 'The Relation of Properties to Structure'. Melbourne, May 1963, Published in Journal of the Australian Institute of Metals, Vol 8 No.4, November 1963.
4	C. Laird G.C. Smith	Crack propagation in high stress fatigue. Phil. Mag. Vol.7, 77, 847 (1962)

Neg. No. C866

Fig.1

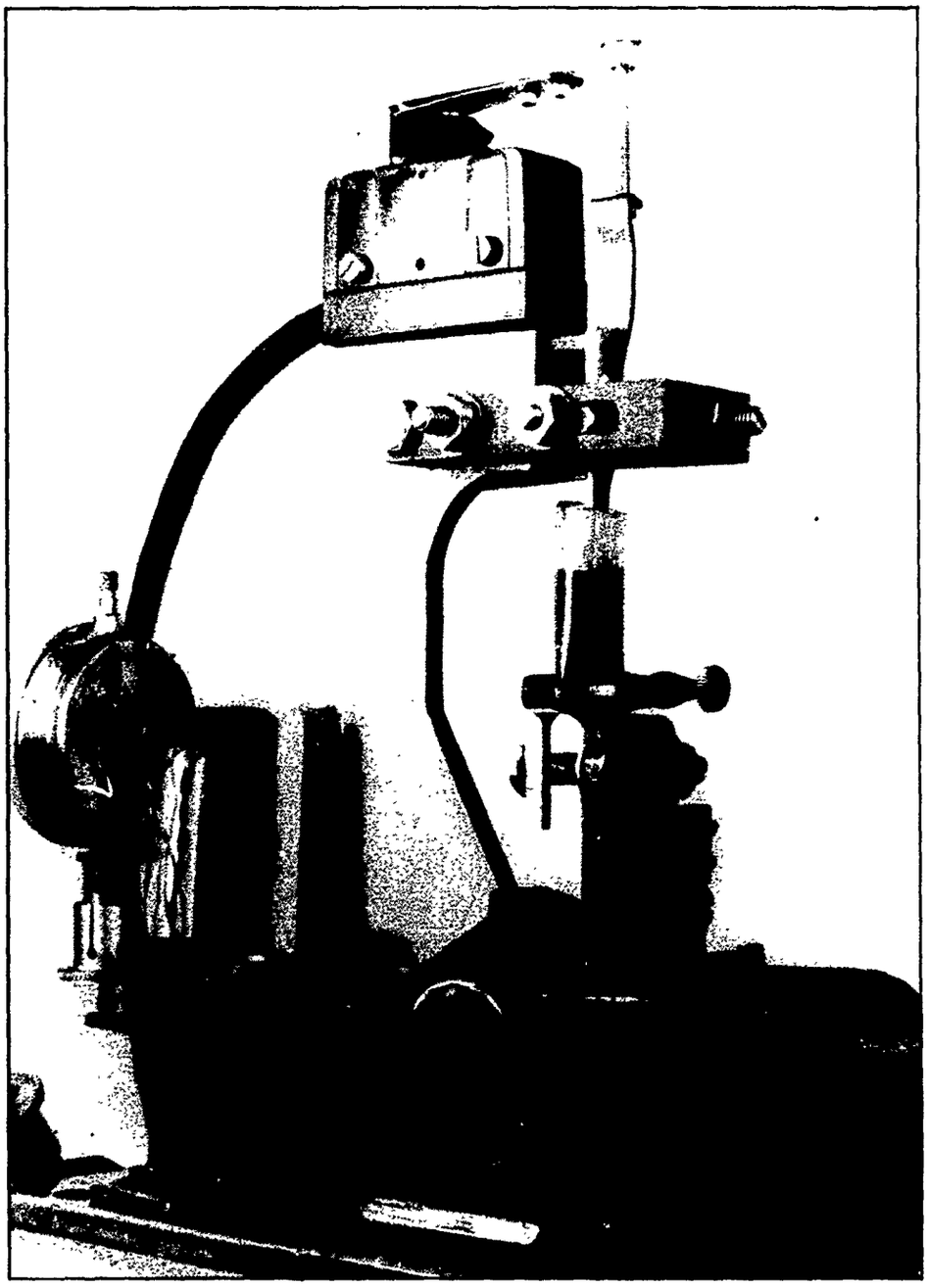

FIG.1 CORROSION FATIGUE ARRANGEMENT ON AVERY SCHENCK MACHINE.

R.65158

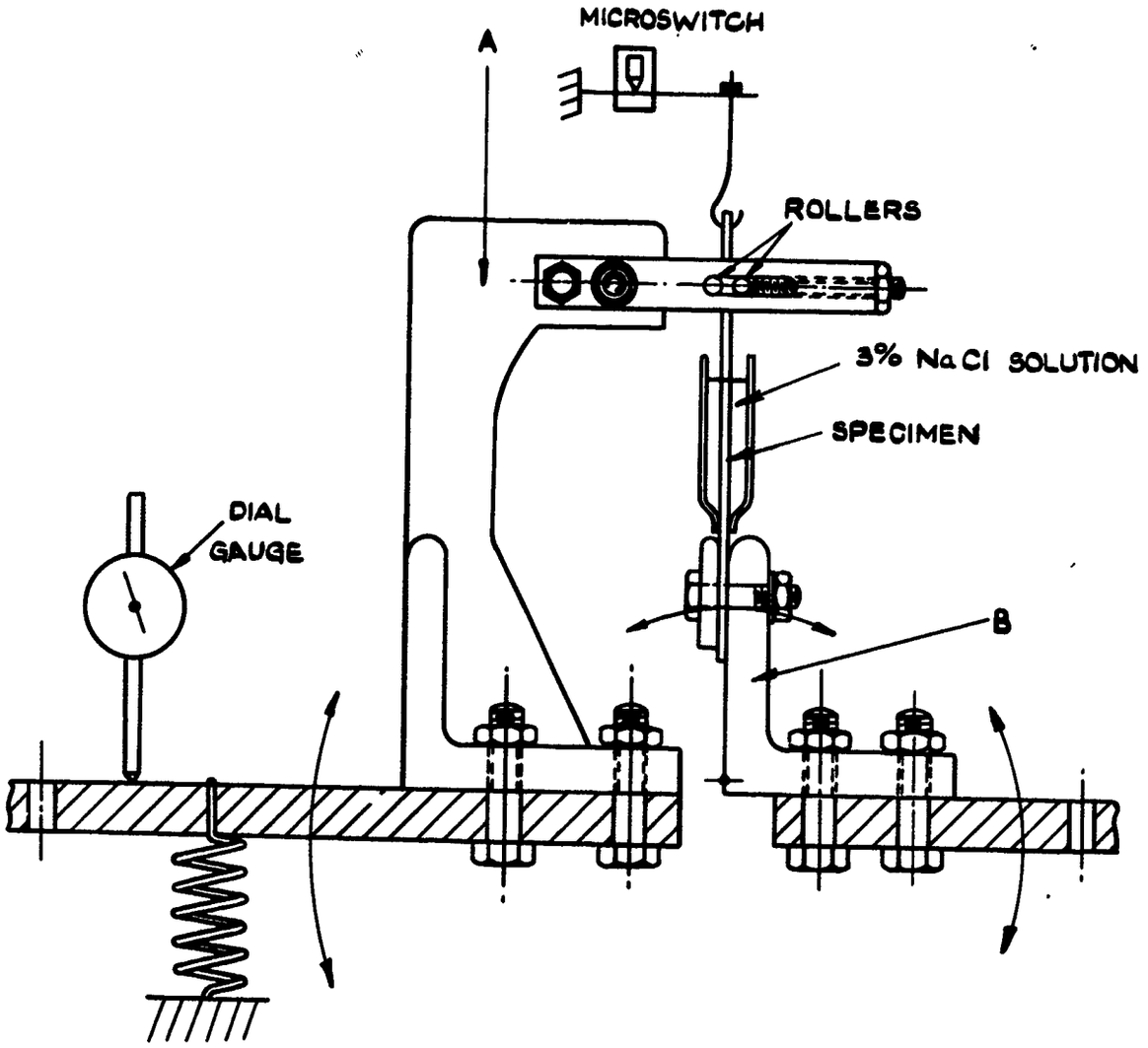

FIG. 2 CORROSION FATIGUE ARRANGEMENT ON AVERY SCHENCK MACHINE

Neg. No. C867

Fig.3

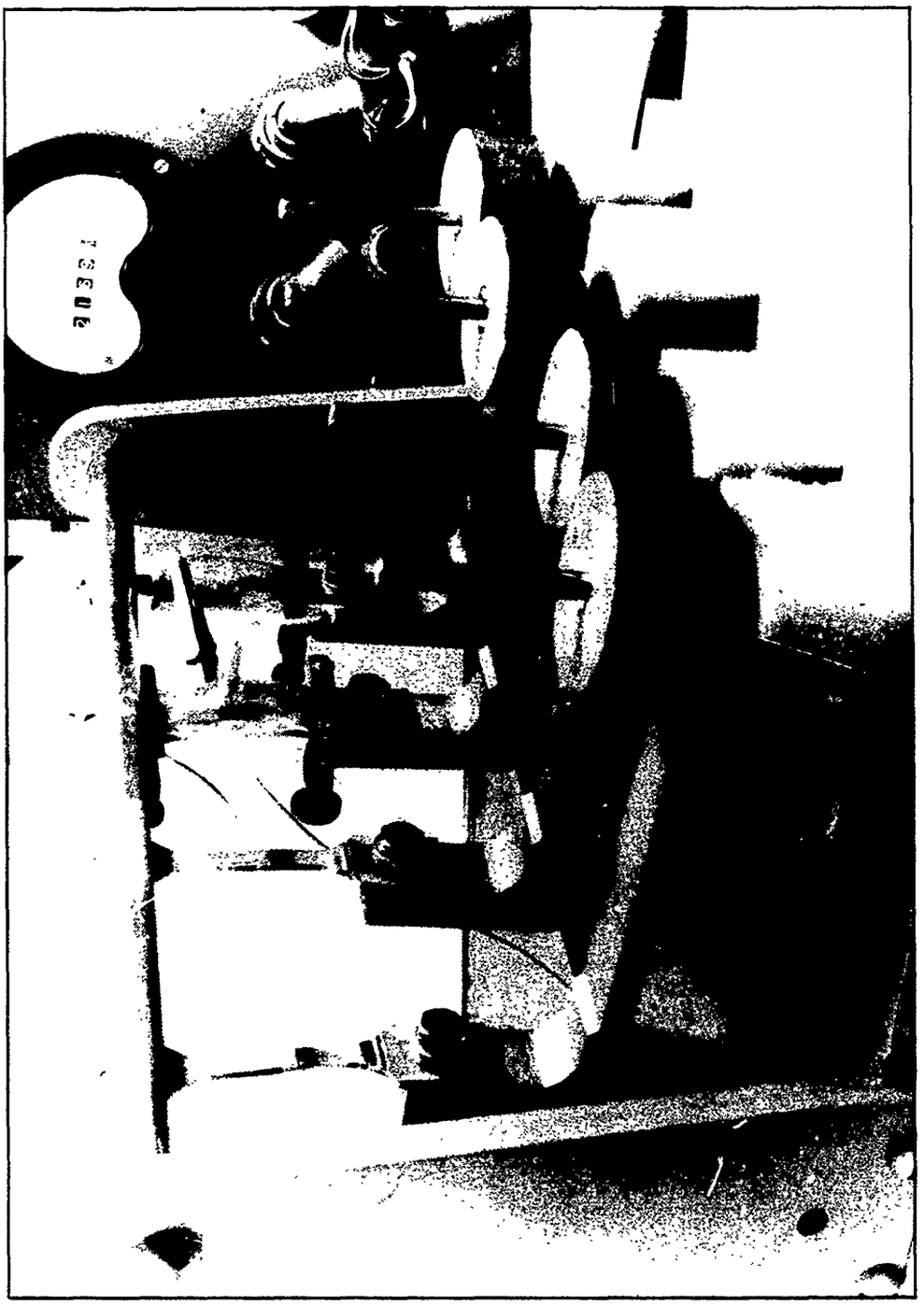

FIG.3 STRESS CORROSION RIG.

R.45158

Fig.4

CPM. R.651

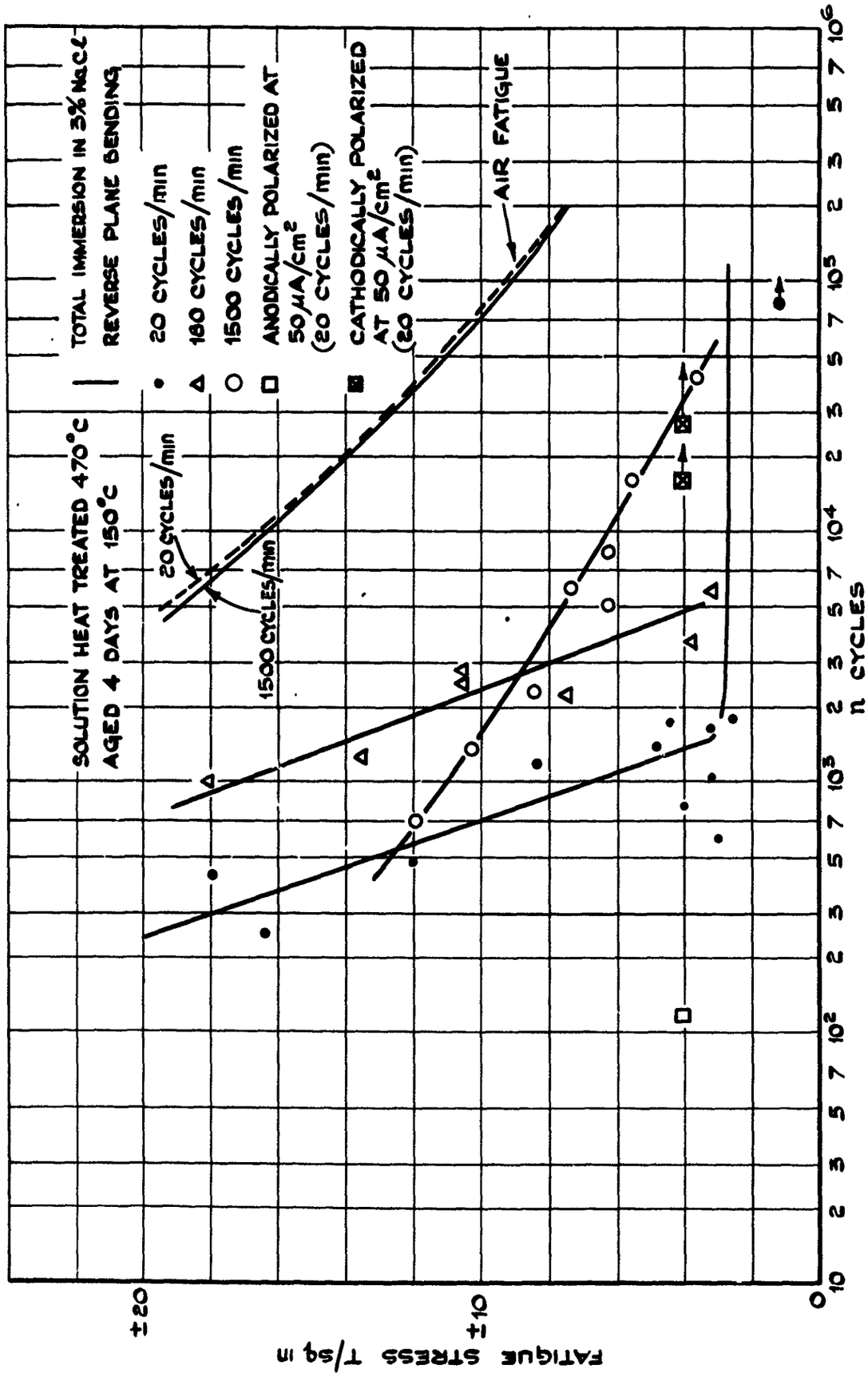

FIG.4 FATIGUE STRESS v LOG n CURVE FOR Al-5Mg-4Zn

Fig.5

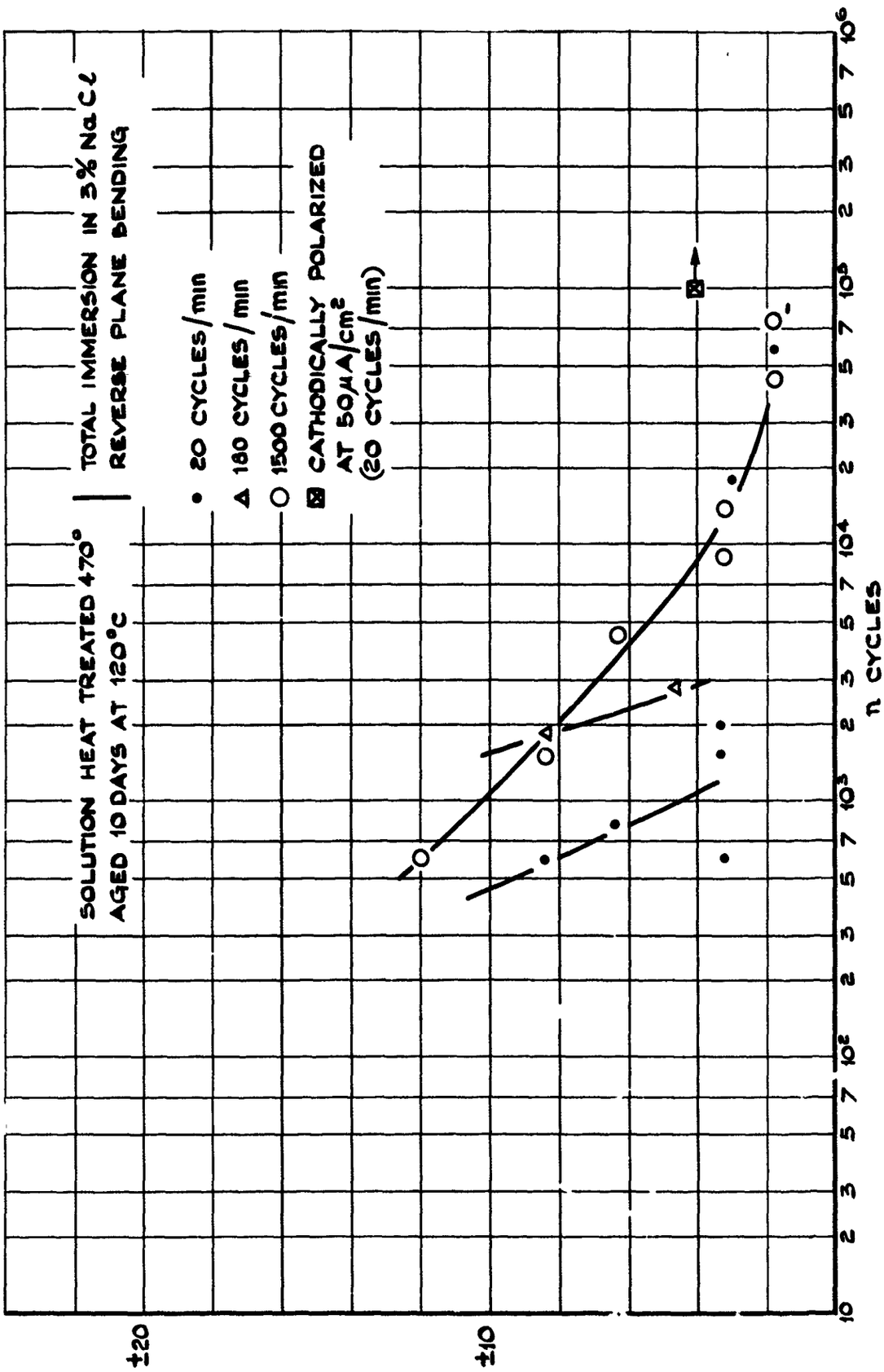

FIG.5 FATIGUE STRESS v LOG n CURVE FOR Al-5Mg-4Zn

Fig.6

CPM/R 653

H 30 AGED 150°C FOR 4 DAYS
L 30 AGED 120°C FOR 10 DAYS

	L 30	H 30
TS t/in²	31·9	30·5
0·1% PS t/in²	28·9	26·0
0·2% PS t/in²	29·7	26·7
0·5% PS t/in²	30·7	27·6
ELONGATION % ON 1"gL	5·0	5·0
$\frac{0.1\%\ PS}{TS}$ RATIO	0·91	0·85

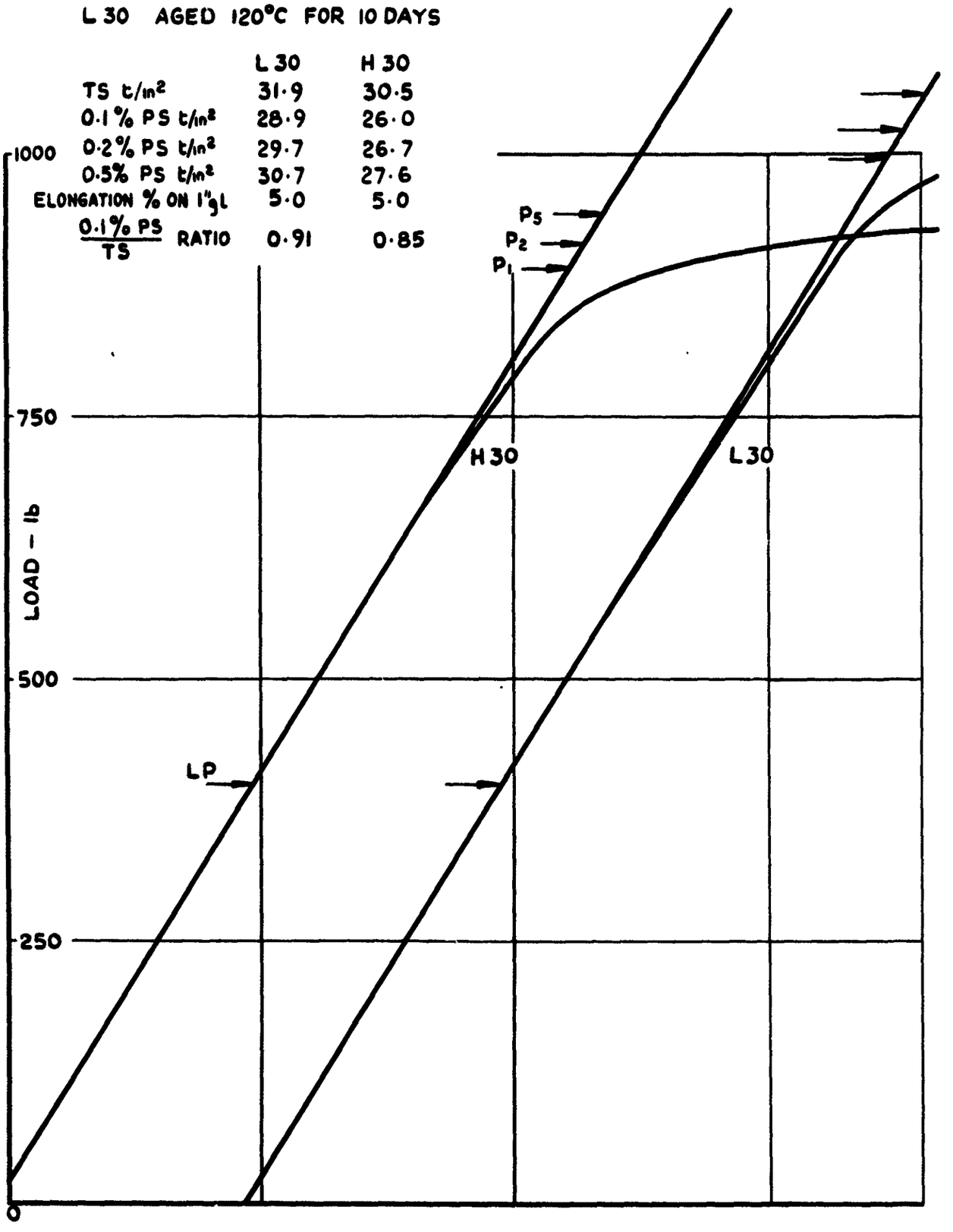

FIG. 6 Al 5 Mg 47n ALLOY: SOLUTION HEAT HEATED AT 470°c AND COLD WATER QUENCHED

Fig.7

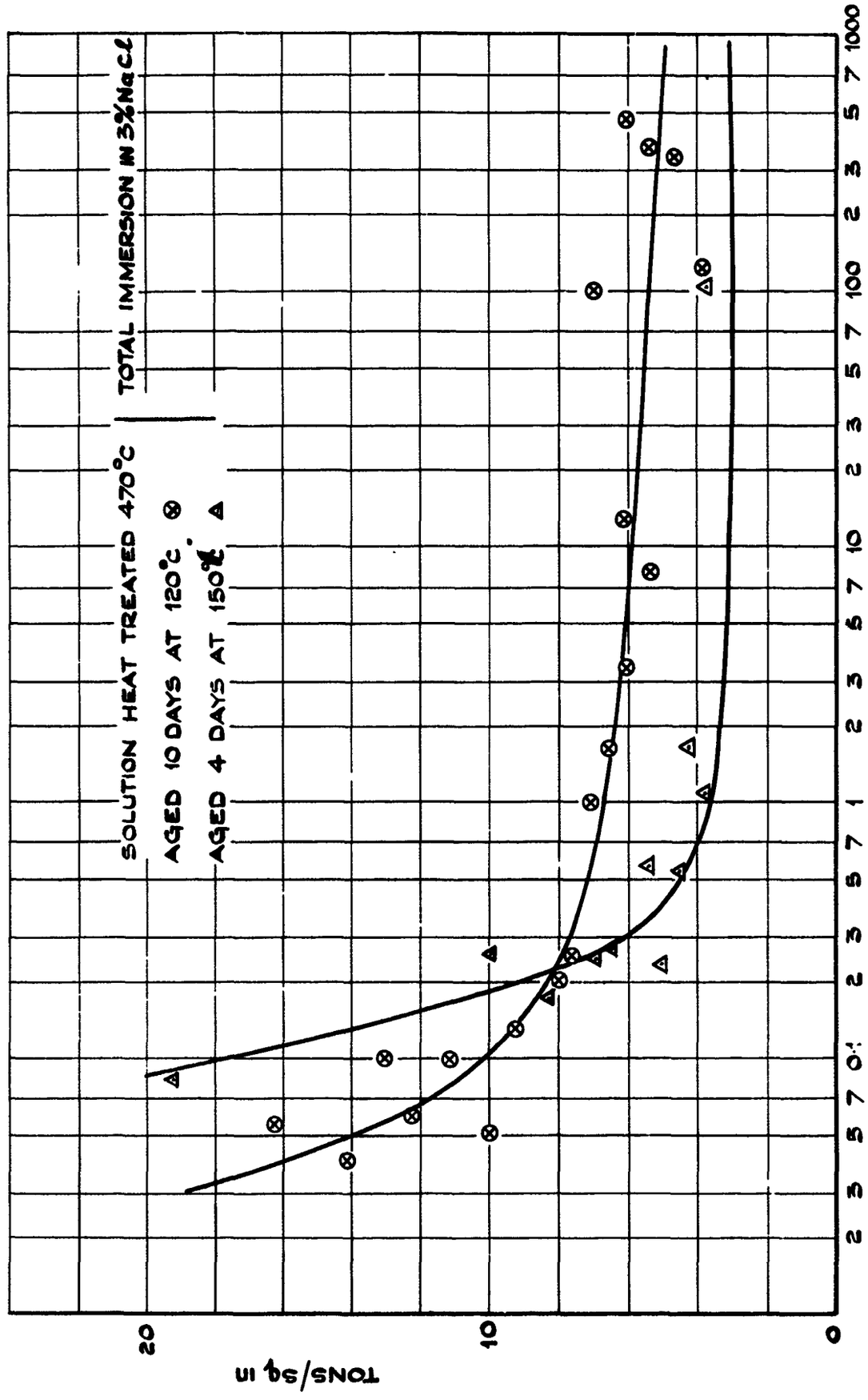

FIG.7a STEADY STRESS v LOG t CURVE FOR Al-5Mg-4Zn

Fig.7

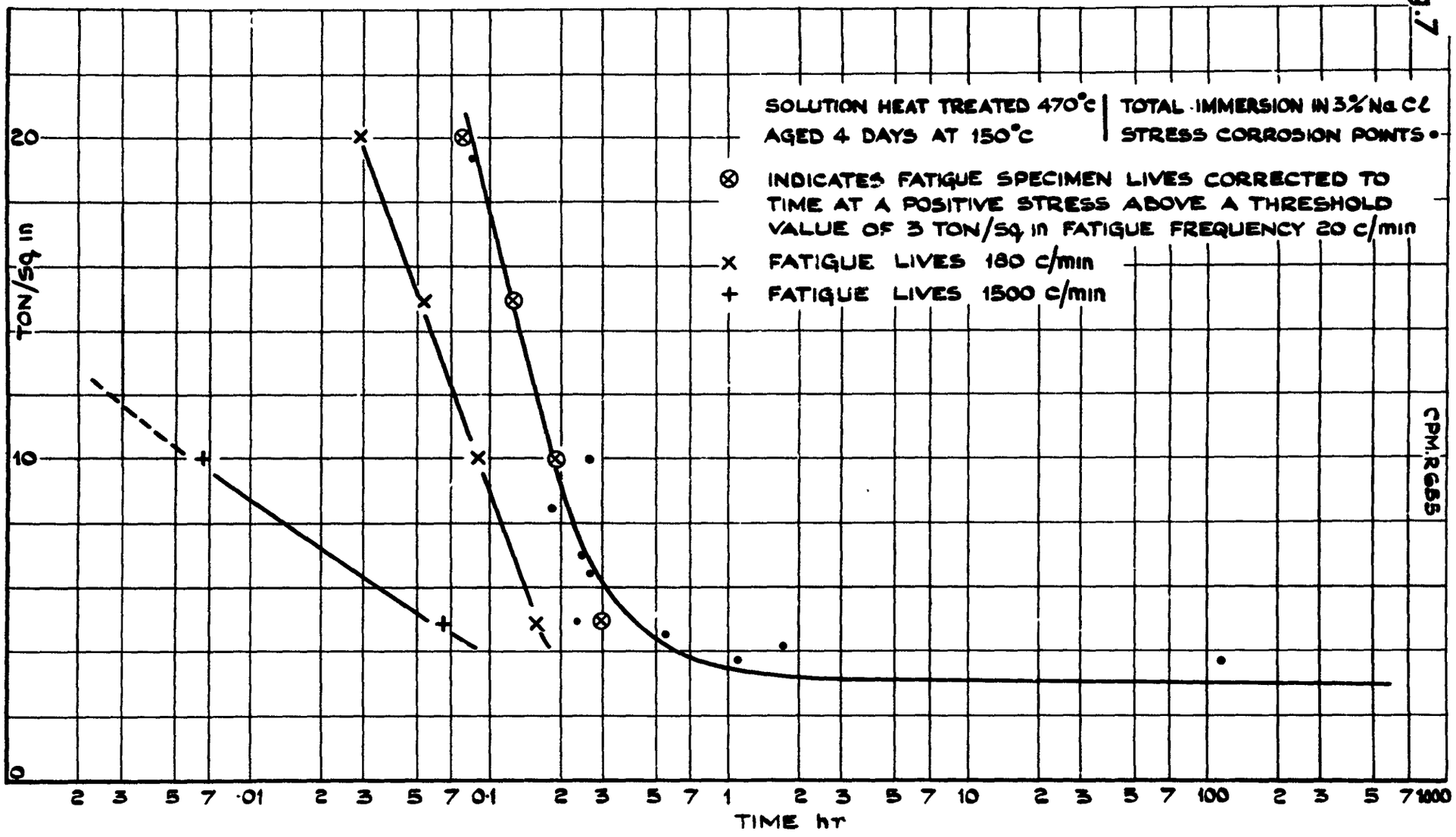

FIG. 7b STEADY STRESS v LOG t CURVE FOR Al-5Mg-4Zn

Fig.8

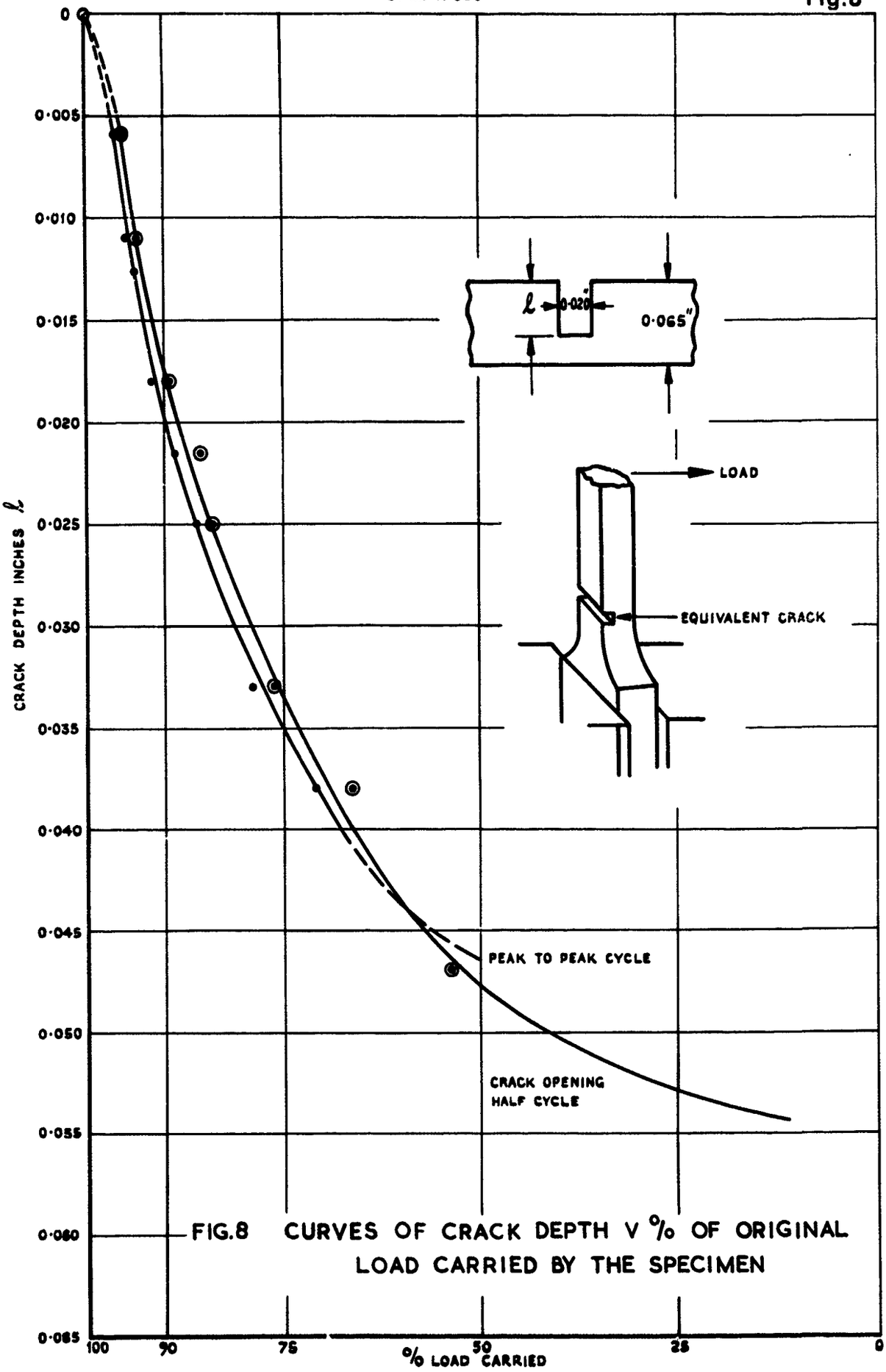

FIG.8 CURVES OF CRACK DEPTH V % OF ORIGINAL LOAD CARRIED BY THE SPECIMEN

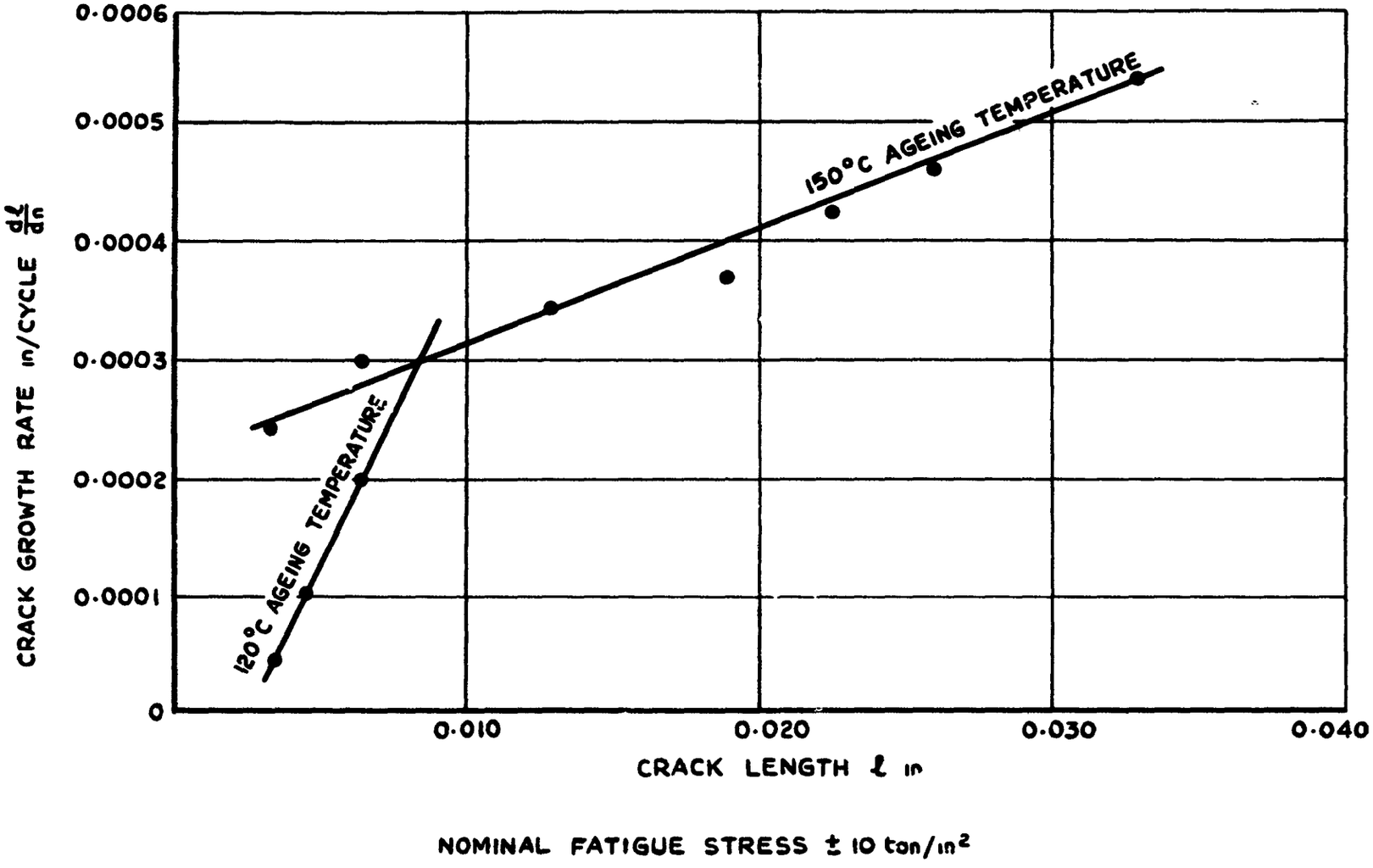

FIG. 9 FATIGUE CRACK GROWTH RATES OF ALUMINIUM 5 MAGNESIUM 4 ZINC ALLOY IMMERSED IN 3% NaCl SOLUTION

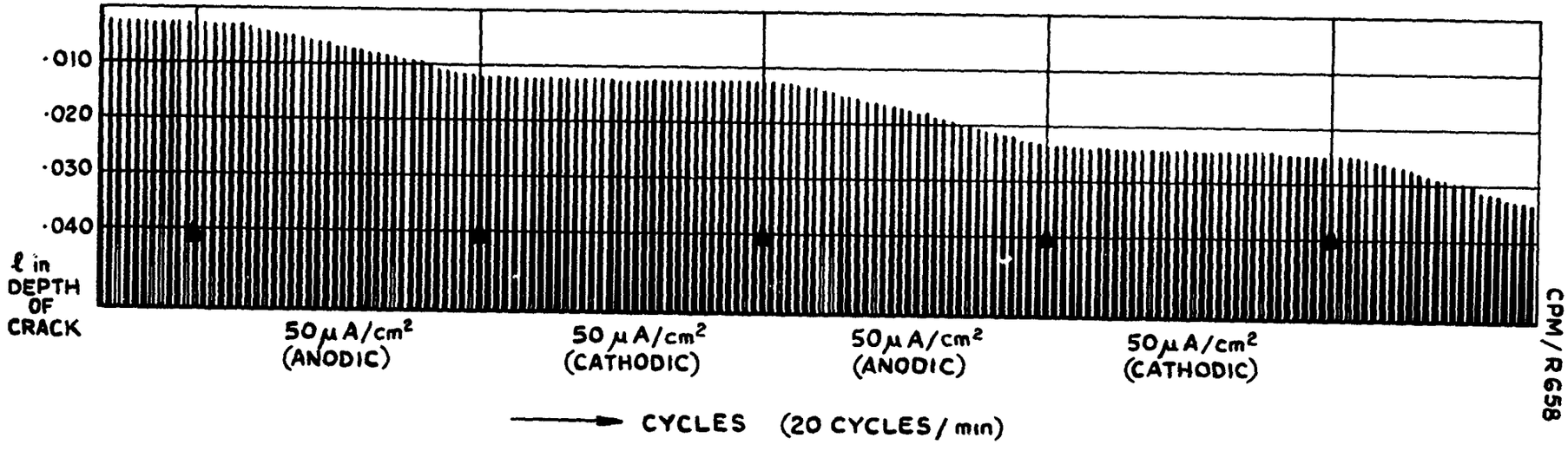

FIG. 10 CHANGES IN CRACK GROWTH RATE WITH IMPRESSED CURRENT

Fig.10

Fig.11&12

Al-5%Mg-4%Zn AGED AT 150°C FOR 4 DAYS.
CATHODICALLY POLARIZED AT 50 $\mu A/cm^2$.

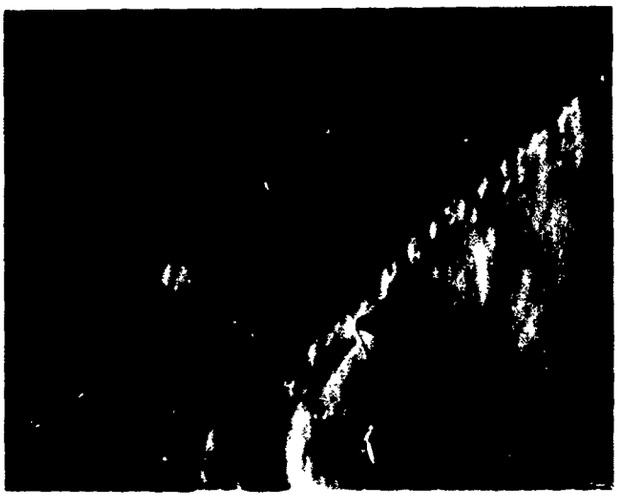

× 1500

FIG.11 'A' INDICATES STRESS CRACKS IN TRANSPARENT HYDROXIDE FILM.

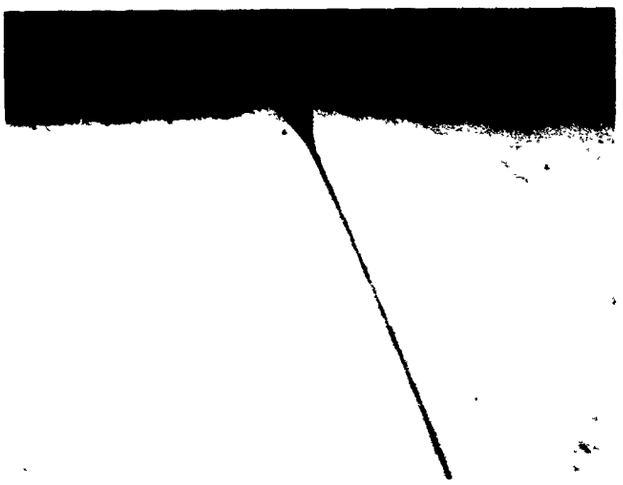

× 1500

FIG.12 SECTION OF ABOVE SPECIMEN SHOWING SURFACE GROOVE AT GRAIN BOUNDARY. [THIS REPRESENTS A NON-PROPAGATING CRACK ORIGIN.]

R.65158

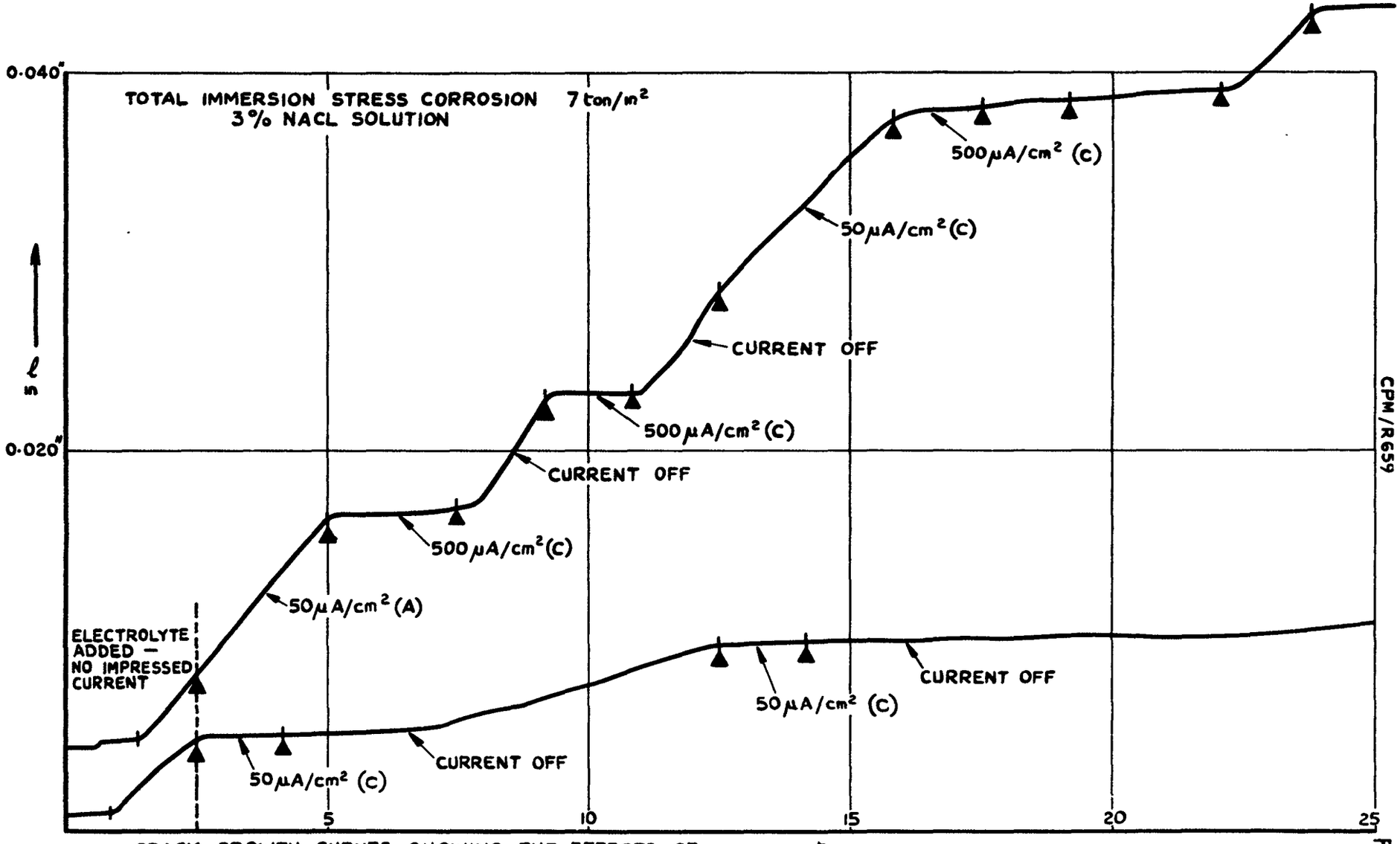

CRACK GROWTH CURVES SHOWING THE EFFECTS OF SEQUENCE AND POLARITY OF IMPRESSED CURRENTS

FIG. 13 Al–5Mg–4Zn AGED 150°c FOR 4 DAYS

Fig.13

Fig.14

CPM.R 660

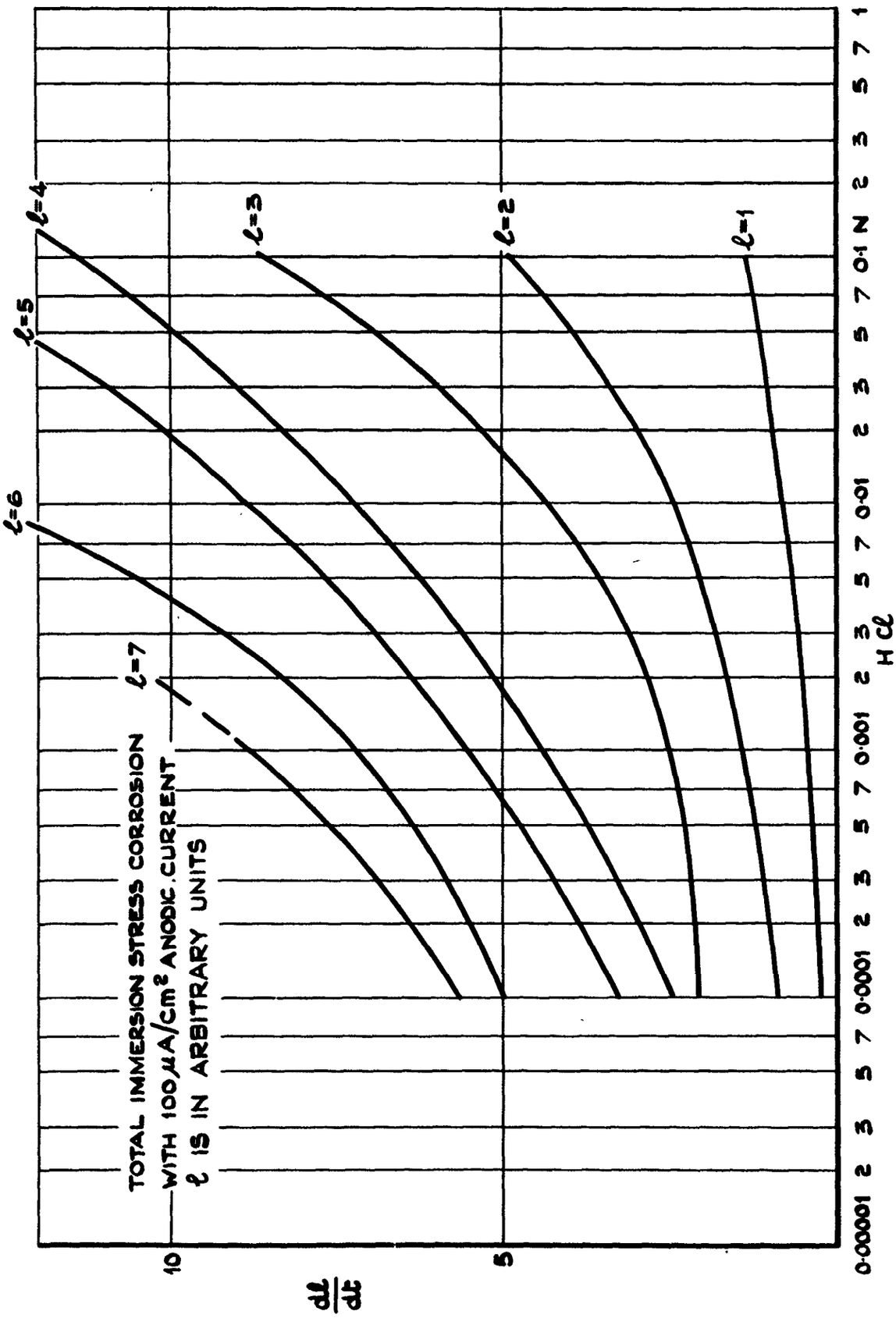

FIG.14 Al-5Mg-4Zn AGED 10 DAYS AT 120°C

Fig.15

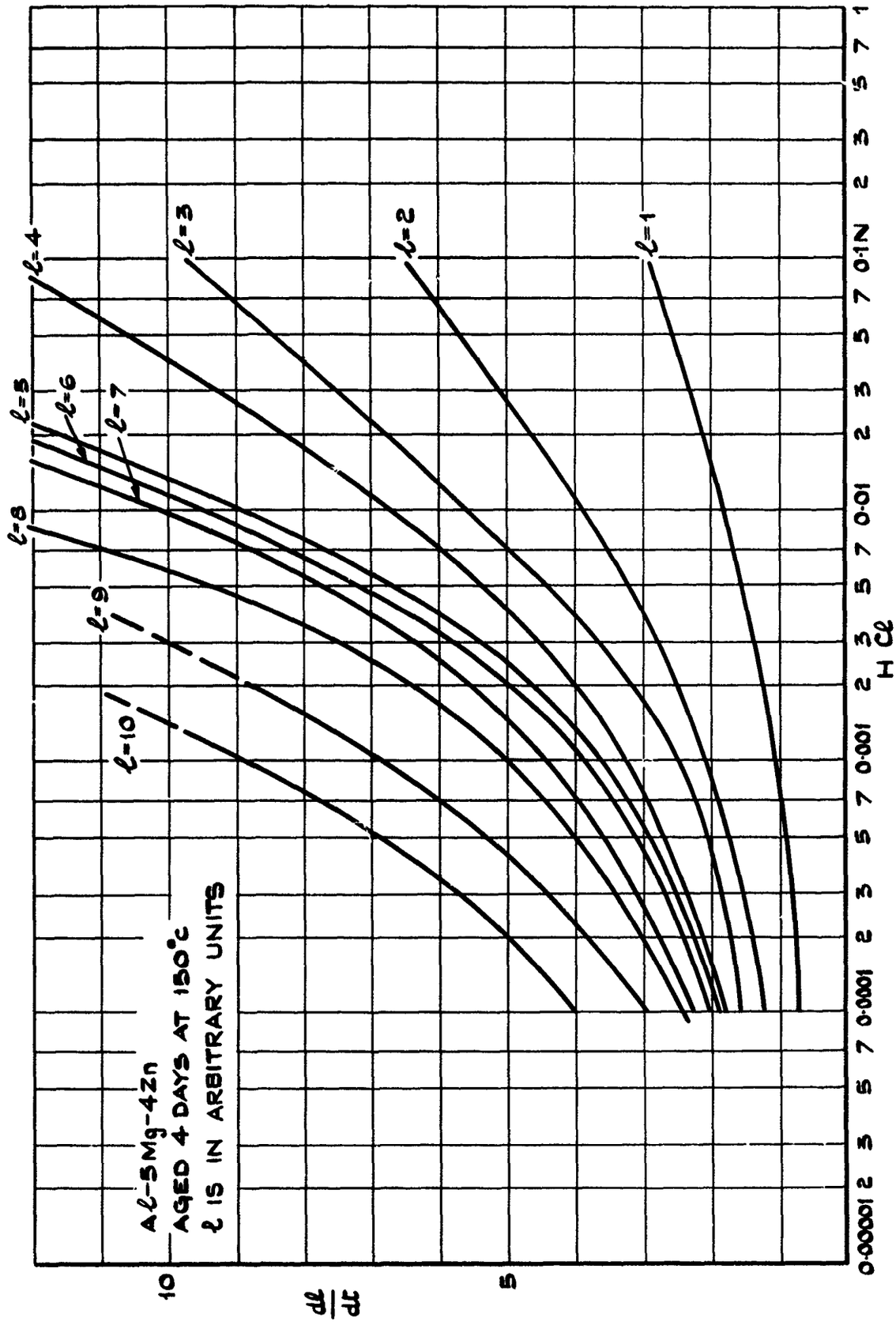

FIG.15 TOTAL IMMERSION STRESS CORROSION WITH 100 μA/cm² ANODIC CURRENT

TOTAL IMMERSION STRESS CORROSION

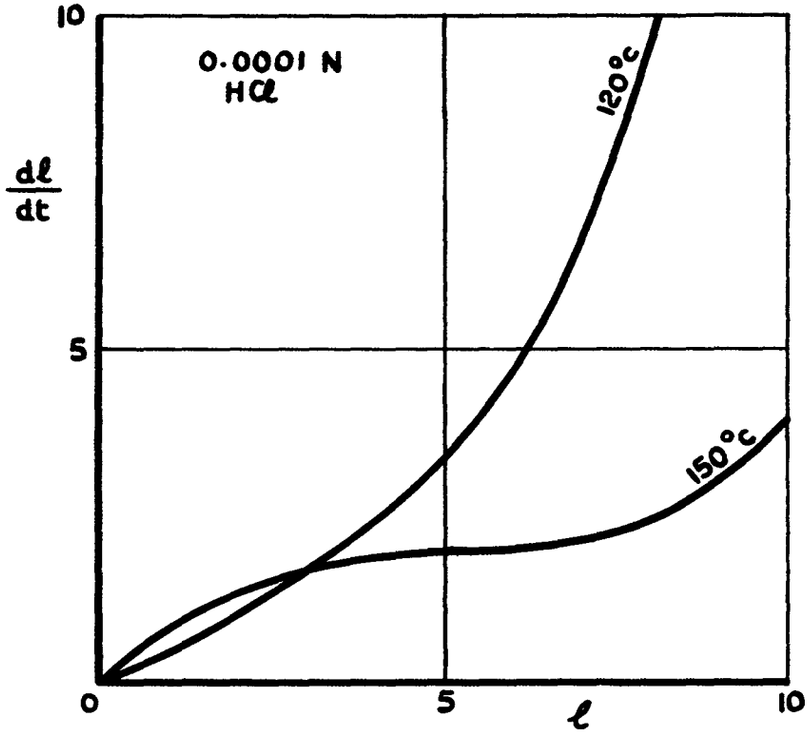

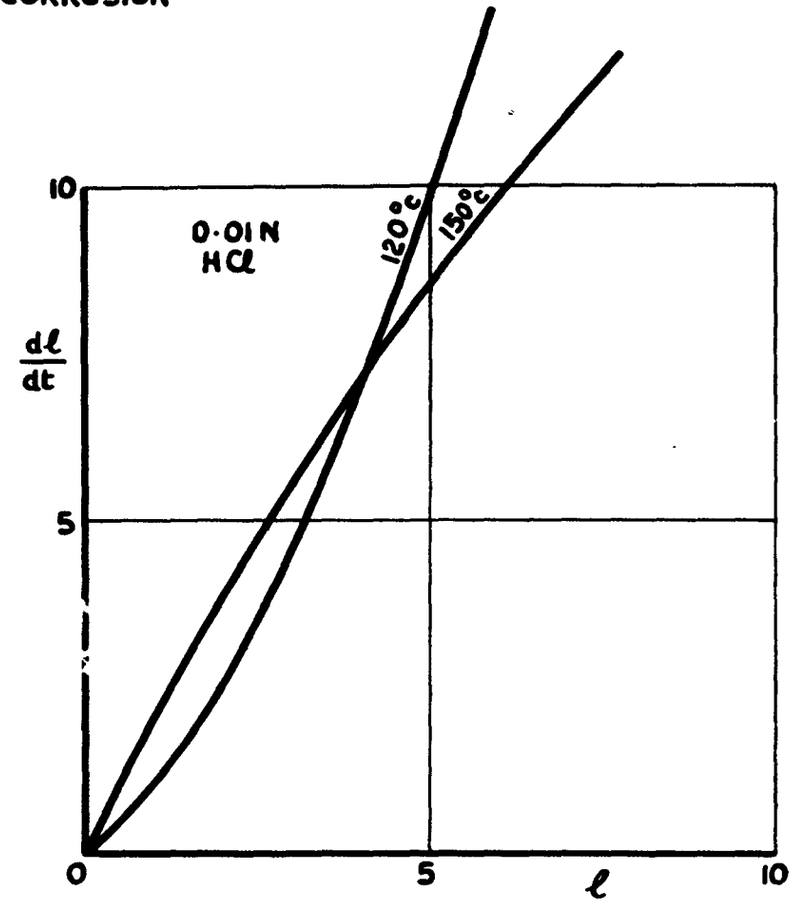

l IS IN ARBITRARY UNITS

FIG. 16 Al – 5Mg – 4Zn AGED TO PEAK HARDNESS AT TEMPERATURES SHOWN

Fig. 16

CPM/R 662

Fig.17

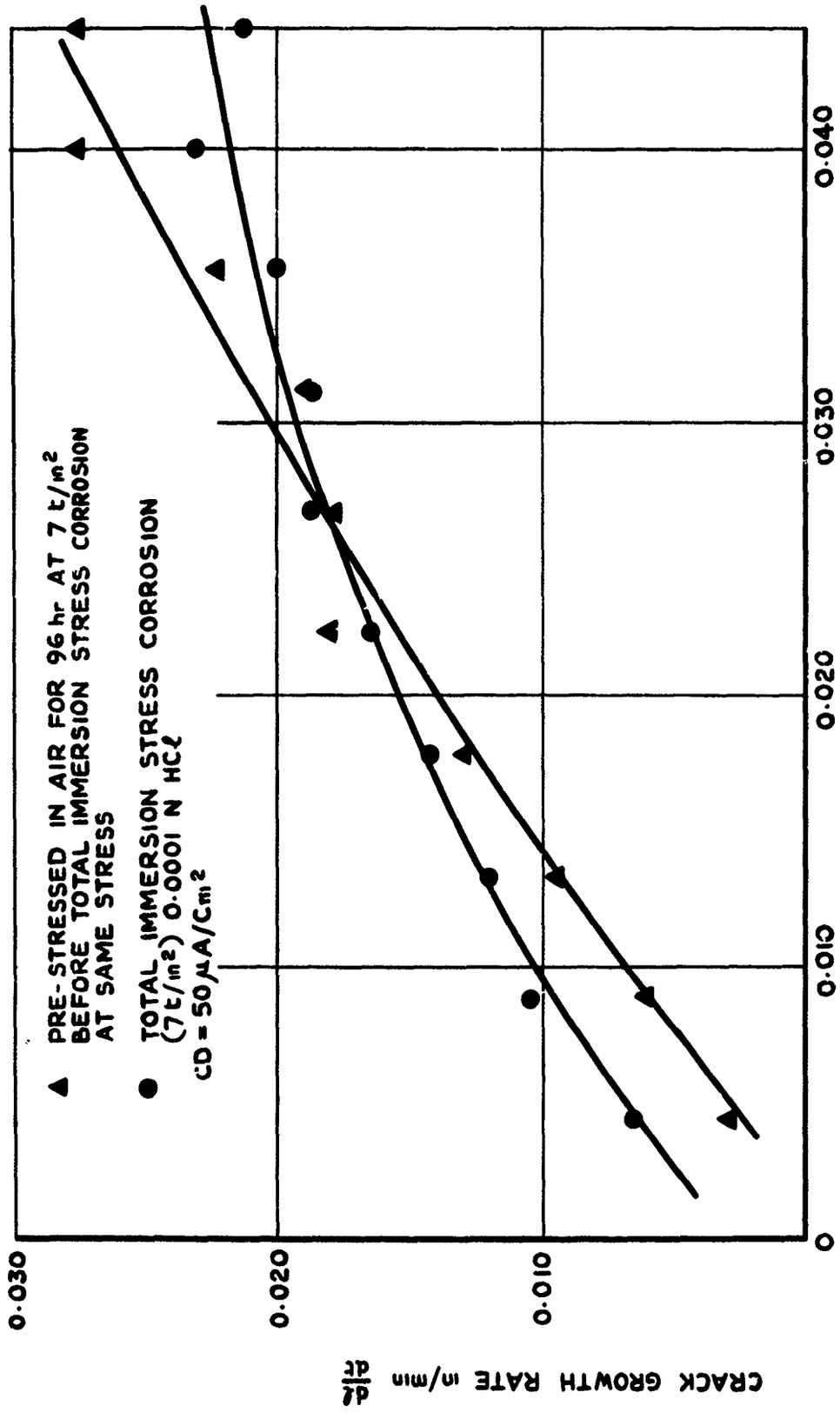

FIG. 17 Al-5% Mg-4% Zn AGED 150°c FOR 4 DAYS

Al-5%Mg-4%Zn AGED AT 150°C FOR 4 DAYS.

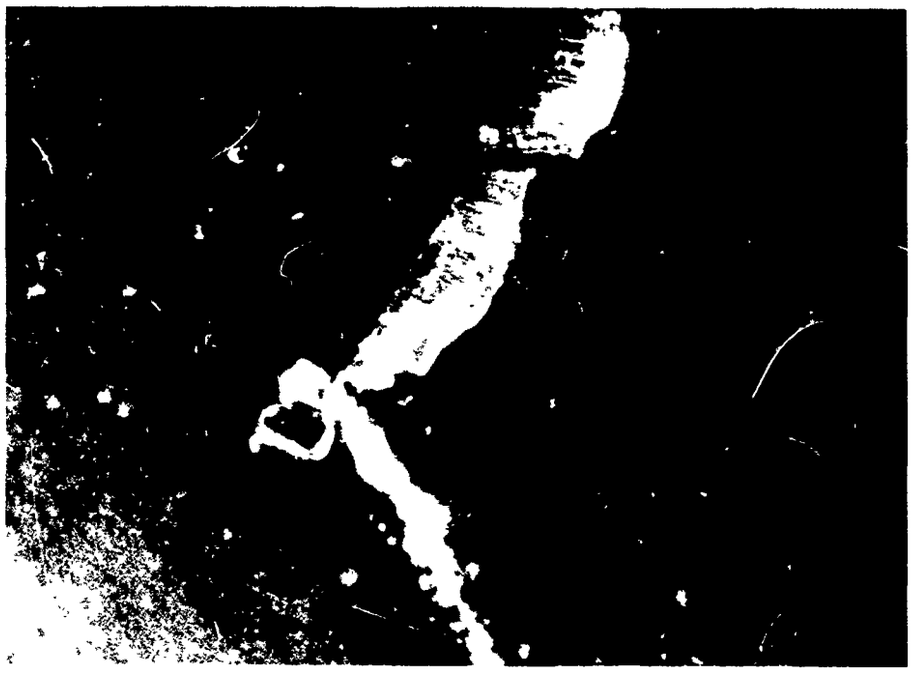

× 500

FIG.18 PHOTOMICROGRAPH (POLARIZED LIGHT) OF EXTRUDED DEBRIS AT GRAIN BOUNDARIES AFTER A PERIOD OF CORROSION FATIGUE.

× 30000

FIG.19 ELECTRON MICROGRAPH (CARBON EXTRACTION REPLICA) OF DEBRIS SHOWN IN FIG.18.

Neg. No. C870

Fig.20

Al-5%Mg-4%Zn AGED AT 150°C FOR 4 DAYS.

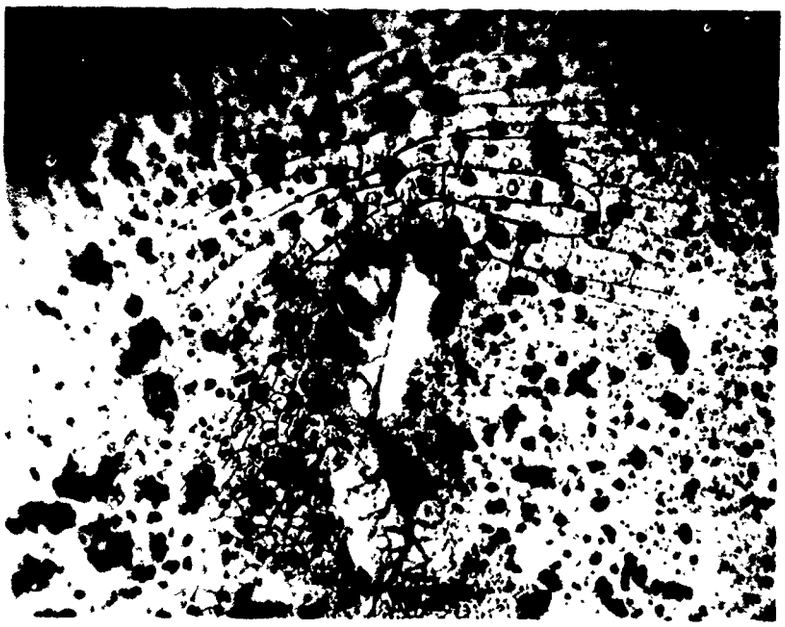

× 250

FIG.20 CRAZED SURFACE FILM FORMED NEAR STRESS CORROSION CRACK ORIGIN.

R.65158

Fig.21-23

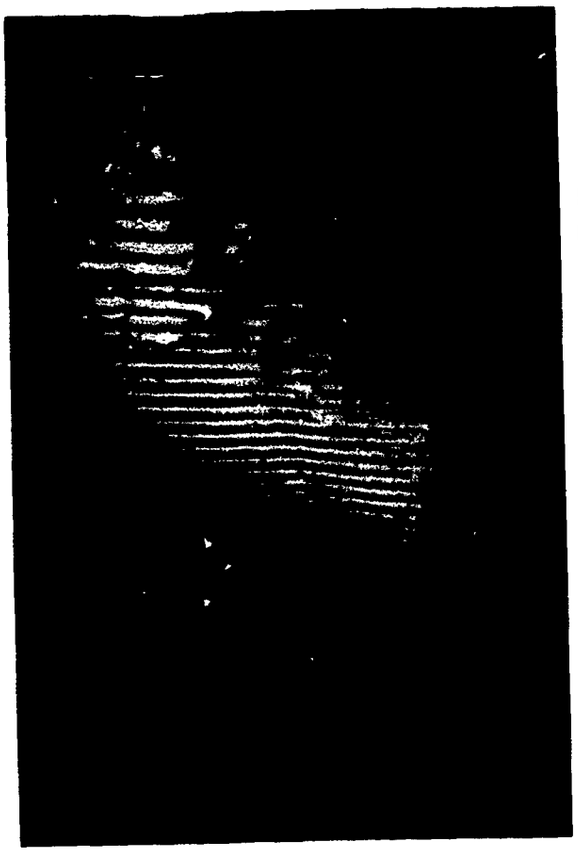

FIG.21 (OPTICAL) × 400

FIG.22 (INTERFEROGRAM) × 800

INTERCRYSTALLINE FRACTURE FACET
WITH FATIGUE STRIATIONS.

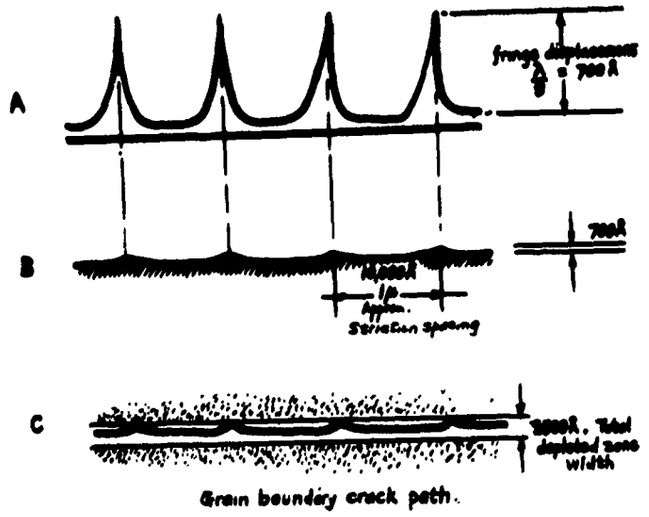

A Interferometric fringes.
B True form of striation contours.
C Crack path in grain boundary.

} Dimensions typical for an Aluminium 5% magnesium 4% zinc experimental alloy

FIG.23 A SCHEMATIC ARRANGEMENT OF GRAIN BOUNDARY FRACTURE.

Fig.24

Al-5%Mg-4%Zn ALLOY AGED 150°C FOR 4 DAYS.

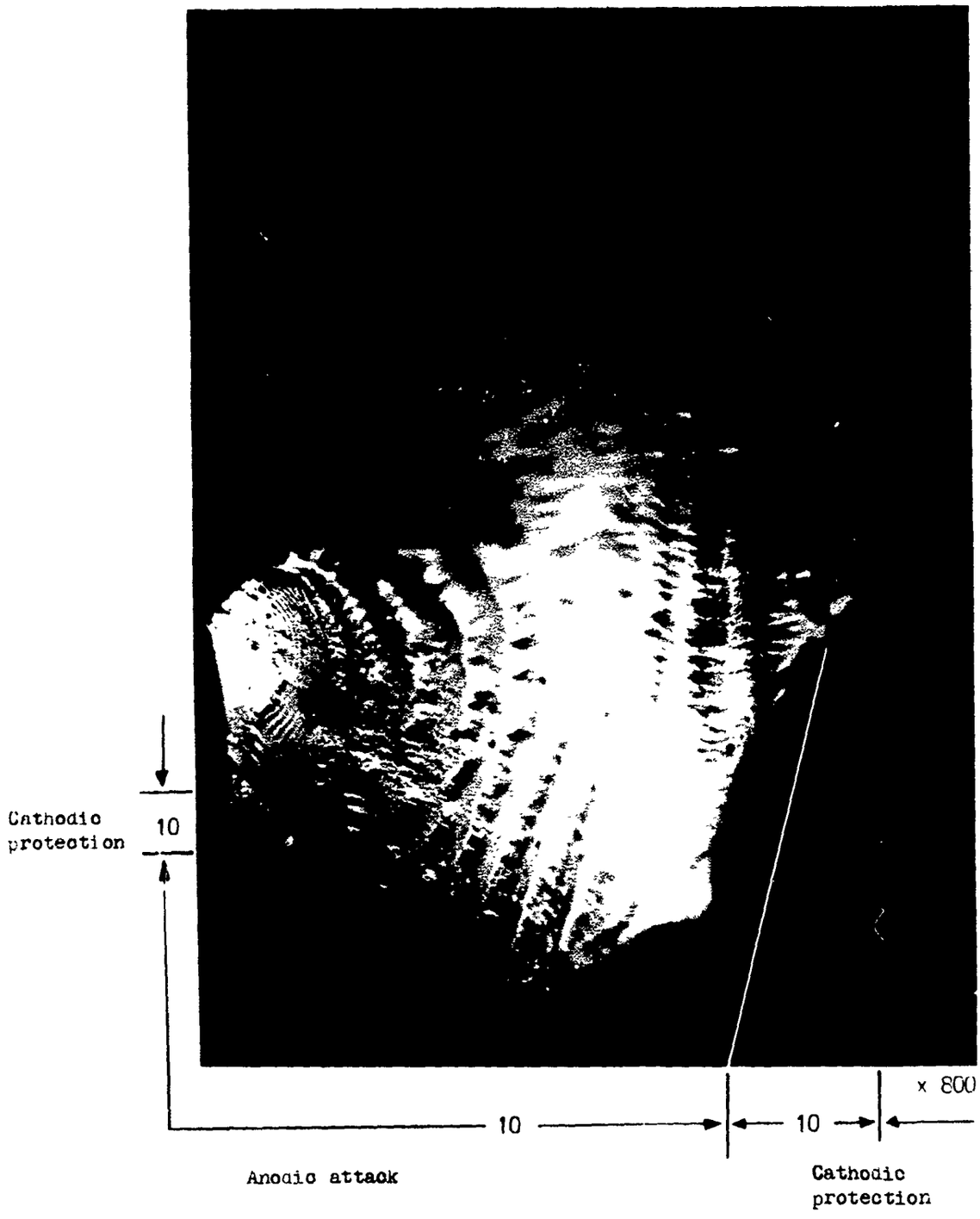

FIG. 24 INTERCRYSTALLINE FRACTURE FACET SHOWING STRIATIONS WITH CHANGING SPACING DEPENDENT ON THE POLARITY OF THE IMPRESSED CURRENT.

R.65158

Fig.25

Al-5%Mg-4%Zn ALLOY AGED AT 150°C FOR 4 DAYS.

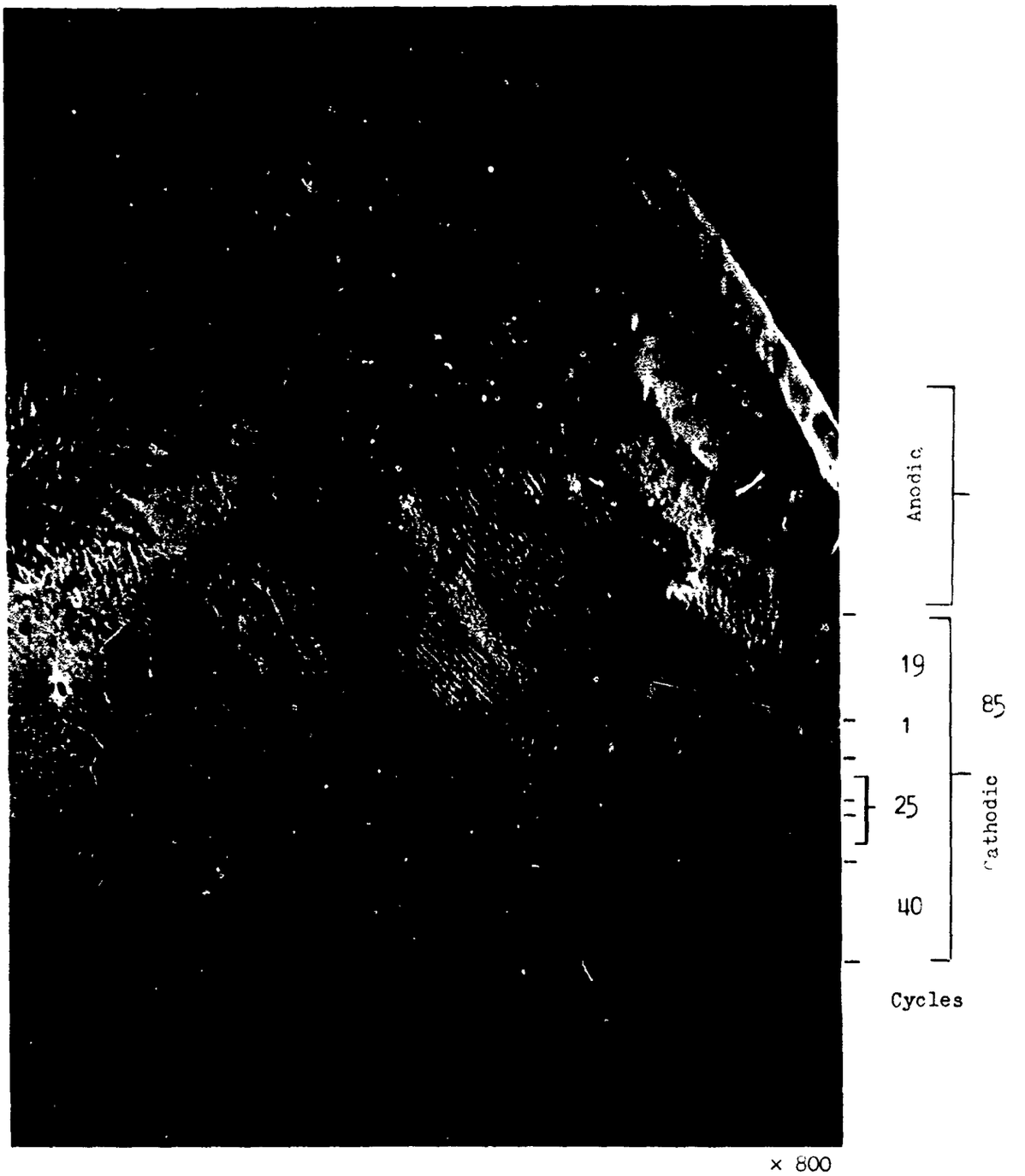

FIG.25 INTERCRYSTALLIC FRACTURE FACET SHOWING STRIATION SPACING CHANGES WITH POLARITY.

R. 65158

Fig.26

Al-5%Mg-4%Zn ALLOY AGED 120°C FOR 10 DAYS.

(a) × 250 (b) × 250

FIG.26 TWO MATING FRACTURE SURFACES SHOWING MARKINGS TYPICAL OF FAST CRACK GROWTH IN THE TERMINAL STAGE OF FATIGUE FRACTURE.
A_1 A_2 INDICATE ONE LARGE STRIATION.
B INDICATES KINK BANDS AS SHOWN IN FIG.27.

Neg No. 875

Fig.27

Al-5%Mg-4%Zn ALLOY AGED 120°C FOR 10 DAYS.

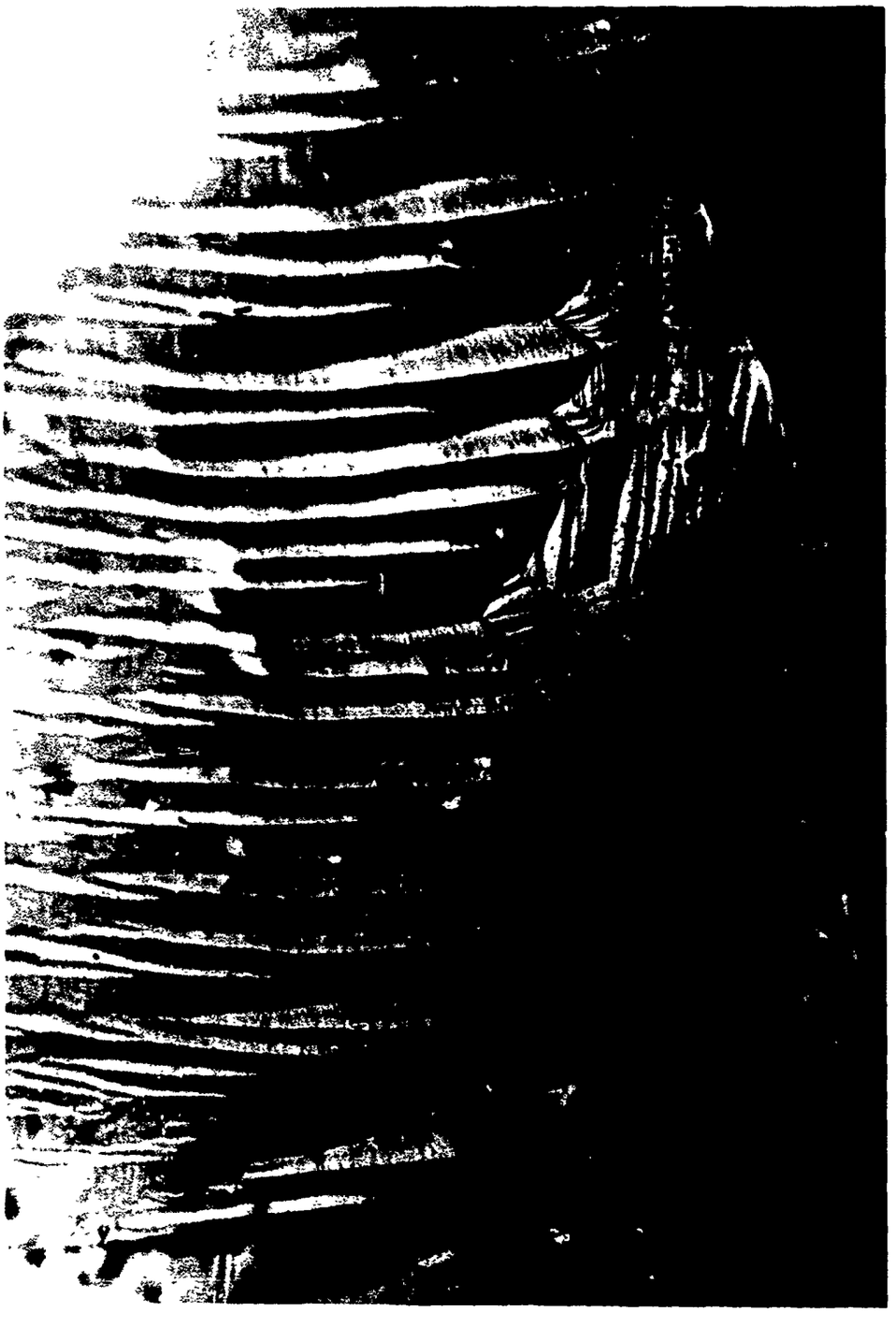

FIG.27 HEAVILY KINKED FRACTURE SURFACE IN TERMINAL REGION OF FATIGUE TEST.

R. 6515B

Fig.28&29

Al-5%Mg-4%Zr ALLOY AGED 120°C FOR 10 DAYS.

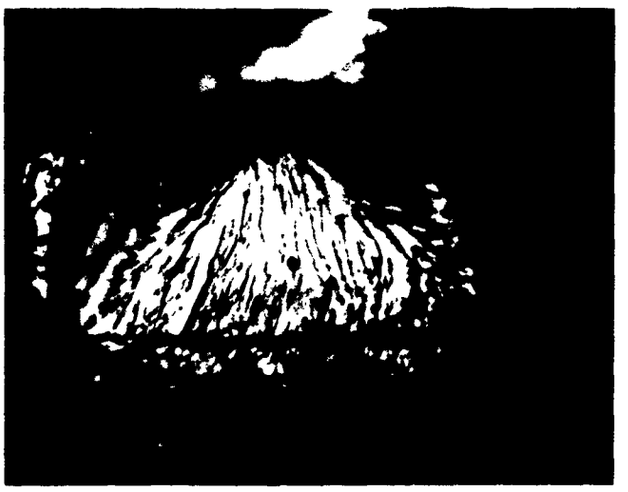

FIG.28 x 250

FIG.29 x 250

FIG.28&29 TWO EXAMPLES OF CLEAVAGE FRACTURE OBSERVED IN THE TERMINAL STAGE OF A STRESS CORROSION FAILURE.

DETACHABLE ABSTRACT CARDS

Forsyth, P.J.E.
Sampson, E.G.F.

669.715.721.5 :
620.194.8 :
620.194.2 :
620.193.27 :
539.219.2

CORROSION FATIGUE AND STRESS CORROSION CRACKING OF AN ALUMINIUM-5% MAGNESIUM-4% ZINC ALLOY TOTALLY IMMERSED IN 3% NaCl AND OTHER CORRODENTS.

Royal Aircraft Establishment Technical Report No. 65158 August 1965

Corrosion fatigue and stress corrosion tests have been done on aluminium-5% magnesium-4% zinc alloy in two conditions of heat-treatment, i.e. aged to peak hardness at 120°C and at 150°C.

The frequency used for most of the fatigue tests was 20 c/min, but comparisons have been made at frequencies of 180 and 1500 c/min. The fatigue endurance at 20 c/min changed only a small amount over a large range of stress. The S/log n curve showed a clearly defined 'knee' and fatigue limit.

(Over)

Forsyth, P.J.E.
Sampson, E.G.F.

669.715.721.5 :
620.194.8 :
620.194.2 :
620.193.27 :
539.219.2

CORROSION FATIGUE AND STRESS CORROSION CRACKING OF AN ALUMINIUM-5% MAGNESIUM-4% ZINC ALLOY TOTALLY IMMERSED IN 3% NaCl AND OTHER CORRODENTS.

Royal Aircraft Establishment Technical Report No. 65158 August 1965

Corrosion fatigue and stress corrosion tests have been done on aluminium-5% magnesium-4% zinc alloy in two conditions of heat-treatment, i.e. aged to peak hardness at 120°C and at 150°C.

The frequency used for most of the fatigue tests was 20 c/min, but comparisons have been made at frequencies of 180 and 1500 c/min. The fatigue endurance at 20 c/min changed only a small amount over a large range of stress. The S/log n curve showed a clearly defined 'knee' and fatigue limit.

(Over)

Forsyth, P.J.E.
Sampson, E.G.F.

669.715.721.5 :
620.194.8 :
620.194.2 :
620.193.27 :
539.219.2

CORROSION FATIGUE AND STRESS CORROSION CRACKING OF AN ALUMINIUM-5% MAGNESIUM-4% ZINC ALLOY TOTALLY IMMERSED IN 3% NaCl AND OTHER CORRODENTS.

Royal Aircraft Establishment Technical Report No. 65158 August 1965

Corrosion fatigue and stress corrosion tests have been done on aluminium-5% magnesium-4% zinc alloy in two conditions of heat-treatment, i.e. aged to peak hardness at 120°C and at 150°C.

The frequency used for most of the fatigue tests was 20 c/min, but comparisons have been made at frequencies of 180 and 1500 c/min. The fatigue endurance at 20 c/min changed only a small amount over a large range of stress. The S/log n curve showed a clearly defined 'knee' and fatigue limit.

(Over)

Forsyth, P.J.E.
Sampson, E.G.F.

669.715.721.5 :
620.194.8 :
620.194.2 :
620.193.27 :
539.219.2

CORROSION FATIGUE AND STRESS CORROSION CRACKING OF AN ALUMINIUM-5% MAGNESIUM-4% ZINC ALLOY TOTALLY IMMERSED IN 3% NaCl AND OTHER CORRODENTS.

Royal Aircraft Establishment Technical Report No. 65158 August 1965

Corrosion fatigue and stress corrosion tests have been done on aluminium-5% magnesium-4% zinc alloy in two conditions of heat-treatment, i.e. aged to peak hardness at 120°C and at 150°C.

The frequency used for most of the fatigue tests was 20 c/min, but comparisons have been made at frequencies of 180 and 1500 c/min. The fatigue endurance at 20 c/min changed only a small amount over a large range of stress. The S/log n curve showed a clearly defined 'knee' and fatigue limit.

(Over)

All crack paths were intercrystalline under both corrosion fatigue and stress corrosion conditions, although air fatigue cracks in this material are mainly transcrystalline.

The slopes of the S/log n curves for 20 and 180 c/min were similar, but the 1500 c/min curve had a smaller slope. This difference was clearly associated with the 'knee' in the 20 c/min curve that was not evident at the higher test frequency.

The effects of both anodic and cathodic polarization have been studied. Marked changes in crack growth rate were observed when a fatigue specimen was alternately made anodic and cathodic in a 3% NaCl solution against either a platinum or aluminium electrode with an externally impressed current. Similar changes in crack growth rate could be obtained with impressed currents under steady stress corrosion conditions. Stress corrosion crack growth rates have been shown to be dependent on the chloride ion concentration of electrolytes used, suggesting a metal dissolution mechanism of stress corrosion in this material.

All crack paths were intercrystalline under both corrosion fatigue and stress corrosion conditions, although air fatigue cracks in this material are mainly transcrystalline.

The slopes of the S/log n curves for 20 and 180 c/min were similar, but the 1500 c/min curve had a smaller slope. This difference was clearly associated with the 'knee' in the 20 c/min curve that was not evident at the higher test frequency.

The effects of both anodic and cathodic polarization have been studied. Marked changes in crack growth rate were observed when a fatigue specimen was alternately made anodic and cathodic in a 3% NaCl solution against either a platinum or aluminium electrode with an externally impressed current. Similar changes in crack growth rate could be obtained with impressed currents under steady stress corrosion conditions. Stress corrosion crack growth rates have been shown to be dependent on the chloride ion concentration of electrolytes used. suggesting a metal dissolution mechanism of stress corrosion in this material.

All crack paths were intercrystalline under both corrosion fatigue and stress corrosion conditions, although air fatigue cracks in this material are mainly transcrystalline.

The slopes of the S/log n curves for 20 and 180 c/min were similar, but the 1500 c/min curve had a smaller slope. This difference was clearly associated with the 'Knee' in the 20 c/min curve that was not evident at the higher test frequency.

The effects of both anodic and cathodic polarization have been studied. Marked changes in crack growth rate were observed when a fatigue specimen was alternately made anodic and cathodic in a 3% NaCl solution against either a platinum or aluminium electrode with an externally impressed current. Similar changes in crack growth rate could be obtained with impressed currents under steady stress corrosion conditions. Stress corrosion crack growth rates have been shown to be dependent on the chloride ion concentration of electrolytes used, suggesting a metal dissolution mechanism of stress corrosion in this material.

All crack paths were intercrystalline under both corrosion fatigue and stress corrosion conditions, although air fatigue cracks in this material are mainly transcrystalline.

The slopes of the S/log n curves for 20 and 180 c/min were similar, but the 1500 c/min curve had a smaller slope. This difference was clearly associated with the 'knee' in the 20 c/min curve that was not evident at the higher test frequency.

The effects of both anodic and cathodic polarization have been studied. Marked changes in crack growth rate were observed when a fatigue specimen was alternately made anodic and cathodic in a 3% NaCl solution against either a platinum or aluminium electrode with an externally impressed current. Similar changes in crack growth rate could be obtained with impressed currents under steady stress corrosion conditions. Stress corrosion crack growth rates have been shown to be dependent on the chloride ion concentration of electrolytes used, suggesting a metal dissolution mechanism of stress corrosion in this material.